

ON Cone Bipolar Cell Axonal Synapses in the OFF Inner Plexiform Layer of the Rabbit Retina

J. Scott Lauritzen, James R. Anderson, Bryan W. Jones, Carl B. Watt, Shoeb Mohammed, John V. Hoang, and Robert E. Marc*

Department of Ophthalmology and Visual Sciences, Moran Eye Center, University of Utah, Salt Lake City, Utah 84132

ABSTRACT

Analysis of the rabbit retinal connectome RC1 reveals that the division between the ON and the OFF inner plexiform layer (IPL) is not structurally absolute. ON cone bipolar cells make noncanonical axonal synapses onto specific targets and receive amacrine cell synapses in the nominal OFF layer, creating novel motifs, including inhibitory crossover networks. Automated transmission electron microscopic imaging, molecular tagging, tracing, and rendering of ~400 bipolar cells reveals axonal ribbons in 36% of ON cone bipolar cells, throughout the OFF IPL. The targets include γ -aminobutyrate (GABA)-positive amacrine cells (γ ACs), glycine-positive amacrine cells (GACs), and ganglion cells. Most ON cone bipolar cell axonal contacts target GACs driven by OFF cone bipolar cells, forming new architectures for generating ON-OFF amacrine cells. Many of these ON-OFF GACs target ON cone bipolar cell axons,

ON γ ACs, and/or ON-OFF ganglion cells, representing widespread mechanisms for OFF to ON crossover inhibition. Other targets include OFF γ ACs presynaptic to OFF bipolar cells, forming γ AC-mediated crossover motifs. ON cone bipolar cell axonal ribbons drive bistratified ON-OFF ganglion cells in the OFF layer and provide ON drive to polarity-appropriate targets such as bistratified diving ganglion cells (bsdGCs). The targeting precision of ON cone bipolar cell axonal synapses shows that this drive incidence is necessarily a joint distribution of cone bipolar cell axonal frequency and target cell trajectories through a given volume of the OFF layer. Such joint distribution sampling is likely common when targets are sparser than sources and when sources are coupled, as are ON cone bipolar cells. *J. Comp. Neurol.* 521:977–1000, 2013.

© 2012 Wiley Periodicals, Inc.

INDEXING TERMS: retina; inner plexiform layer; connectomics; circuitry; neural network; bipolar cell; axonal ribbon; axonal cistern; amacrine cell; bistratified diving ganglion cell; intrinsically photosensitive ganglion cell; crossover inhibition; within channel inhibition; ON-OFF cross-talk; functional network; structure–function; network topology

Structure–function relationships have been explored in the retina for over a century. Ramón y Cajal (1892) observed differential bipolar cell stratification in the inner plexiform layer (IPL) and suspected direct structure–function correlations. Indeed, it has long been established that ON and OFF channels occupy distinct domains within the mammalian IPL, with OFF cells that depolarize to light decrements stratified in the distal 40% of the IPL and ON cells that depolarize to light increments stratified in the proximal 60% of the IPL (Famiglietti et al., 1977; Famiglietti and Kolb, 1976; MacNeil et al., 2004; Wässle et al., 2009; Werblin and Dowling, 1969). Nevertheless, examples of nominal cone bipolar cells breaking the mammalian IPL stratification rules were recently reported (Anderson et al., 2011a; Dumitrescu et al., 2009; Hoshi et al., 2009). Type 6, and possibly type 7 or 8, ON cone

bipolar cells in mouse, and calbindin-positive layer 4/5 stratifying ON cone bipolar cells in rabbit, have been demonstrated targeting tyrosine hydroxylase-positive cells (TH1s), M1-type intrinsically photosensitive retinal ganglion cells (ipRGCs), and bistratified diving ganglion cells (bsdGCs) in stratum 1 of the IPL (Dumitrescu et al., 2009;

Grant sponsor: National Institutes of Health; Grant number: EY02576 (to R.E.M.); Grant number: EY015128 (to R.E.M.); Grant number: EY014800 Vision Core (to R.E.M.); Grant sponsor: National Science Foundation; Grant number: 0941717 (to R.E.M.); Grant sponsor: Research to Prevent Blindness (RBP; to Moran Eye Center); RPB Career Development Award (to B.W.J.); Grant sponsor: Thome Foundation grant for AMD Research (to B.W.J.).

*CORRESPONDENCE TO: Robert E. Marc, Ophthalmology and Vision Sciences, Moran Eye Center, University of Utah, Salt Lake City, UT 84132. E-mail: robert.marc@hsc.utah.edu

Received April 25, 2012; Revised October 3, 2012; Accepted October 4, 2012

DOI 10.1002/cne.23244

Published online October 8, 2012 in Wiley Online Library (wileyonlinelibrary.com)

© 2012 Wiley Periodicals, Inc.

Hoshi et al., 2009), thus representing an accessory ON input to the OFF IPL layers. These ribbon contacts appear in two varieties: en passant, occurring inside the main bipolar cell descending axons, and branched, occurring from small processes that branch from the main descending axon (see Fig. 2). Anderson et al. (2011a) demonstrated by automated transmission electron microscopic (ATEM) imaging that presynaptic ribbon and postsynaptic conventional synaptic ultrastructures existed at axonal ribbon locations, but characterization of their cognate networks was incomplete.

Indirect evidence exists suggesting that different ON cone bipolar cell types might communicate in the OFF IPL. First, in previous confocal imaging studies (Hoshi et al., 2009), only 23% of bsdGCs were apposed to calbindin-positive bipolar cells, but most bsdGC spines were apposed to ribeye puncta. This indicates that the remaining ribbons must be associated with other bipolar cell types. Also, many nonmammalian bipolar cell classes are multistratified, with axonal outputs in both the OFF and the ON sublayers (Kolb, 1982; Pang et al., 2004; Ramón y Cajal, 1892; Scholes, 1975; Scholes and Morris, 1973; Sherry and Yazulla, 1993; Wong and Dowling, 2005). Moreover, infrequent reports of mammalian bistratified bipolar cells exist (Calkins et al., 1998; Famiglietti, 1981; Jeon and Masland, 1995; Kolb et al., 1990, 1992; Linberg et al., 1996; Mariani, 1982; McGuire et al., 1984). These results impelled us to comprehensively classify ON cone bipolar cells that synapse in the OFF sublayer of the IPL.

In addition to the previously identified axonal ribbon targets, unknown targets with distinctive morphologies and ultrastructural elements were observed in retinal connectome RC1 (Anderson et al., 2011a). This strongly suggested additional cell types as targets. Axonal cisterns associated with postsynaptic densities were also discovered in the axons of ON cone bipolar cells (Anderson et al., 2011a) and are thus possible contributors to accessory ON networks. Sparse reports of rod bipolar cell axonal ribbons exist, implicating them as candidates for providing the ON input to ipRGCs, yet we demonstrate

that rod bipolar cell axonal ribbons are not spatially coincident with ipRGCs and so cannot be responsible for ipRGC ON drive.

Electrophysiology with pharmacological blockade has revealed glycinergic cross-talk between ON and OFF channels at every synaptic tier in the retina, referred to as “crossover inhibition” (Chavez and Diamond, 2008; Chen et al., 2011; Liang and Freed, 2010; Manookin et al., 2008; Molnar et al., 2009; Roska et al., 2006; Werblin, 2010). Multistratified GACs are implicated as the source, yet the network topologies responsible remain a matter of speculation. Crossover inhibition has been posited to achieve a range of functions, including fidelity restoration of photic drive distorted by glutamate synapse nonlinearities, which would otherwise constrain OFF channels to negative contrast processing (Liang and Freed, 2010; Molnar et al., 2009; Werblin, 2010). Given that some of the targets of axonal ribbon synapses are glycine-positive amacrine cells (GACs), ON–OFF crossover is one possible function of this accessory input. We show that crossover inhibition can definitely arise from accessory ON bipolar cell networks.

γ -Aminobutyrate (GABA)-positive amacrine cells (γ ACs) mediate feedback, nested feedback, and feedforward networks throughout the retina, yet the reasons for the great diversity of types (wide-field, narrow-field, mono-, and multistratified) remain a mystery (Marc and Liu, 2000; Wagner and Wagner, 1988). We show examples of wide-field, OFF layer, monostratified γ AC processes postsynaptic to ON cone bipolar cell axonal ribbons and presynaptic to both ON and OFF cone bipolar cells, arguing for the existence of γ AC-mediated within- and cross-channel inhibition in addition to GAC-mediated within- and cross-channel inhibition. Many instances of GAC-mediated and γ AC-mediated crossover inhibition motifs have been identified in RC1 that do not involve axonal ribbons (data not shown); these will be the subject of future studies.

In summary, ON cone bipolar cells participate in accessory ON input throughout the OFF sublayer of IPL, targeting not only the previously characterized ipRGCs and bsdGCs but also newly identified targets. As yet unknown targets exist in RC1, some of which may be the sparse TH1 axonal cell dendrites reported by Dumitrescu et al. (2009) and Hoshi et al. (2009). Additionally, preliminary data reveal that 68 of 97 (70.1%) measured ON cone bipolar cells contain one or more postsynaptic densities (PSDs) to amacrine cell input in the OFF IPL, and recently discovered axonal cisterns appear in 55 of 113 (48.7%) ON cone bipolar cell axons measured thus far. This specificity enhances the likelihood that accessory ON networks are evolved strategies rather than systemic oddities. Furthermore, such networks are not readily predicted by physiological techniques. ON cone bipolar cell axonal ribbons inject both

Abbreviations

INL	Inner Nuclear Layer
IPL	Inner Plexiform Layer
GCL	Ganglion Cell Layer
GAC	Glycine-positive Amacrine Cell
γ AC	GABA-positive Amacrine Cell
A _I AC	A1 Amacrine Cell = A17 Amacrine Cell
A _{II} AC	AII Amacrine Cell
ipRGC	Intrinsically Photosensitive Retinal Ganglion Cell
bsdGC	Bistratified Diving Ganglion Cell
>	Sign-Conserving Synapse
≥	Sign-Inverting Synapse
::	Gap Junction
GABA _A R	GABA _A Receptor
GABA _C R	GABA _C Receptor
glyR	Glycine Receptor

TABLE 1.
Primary Antibodies Used in This Study¹

Antibody	Immunogen, host species	Source	Dilution used
AGB	BSA–glutaraldehyde (1-amino-4-guanidobutane) conjugate, rabbit	Signature Immunologics B100/rabbit polyclonal	1:4,000
GABA	BSA–glutaraldehyde (4-aminobutyrate) conjugate, rabbit	Signature Immunologics YY100/rabbit polyclonal	1:32,000
Glycine	BSA–glutaraldehyde (glycine) conjugate, rabbit	Signature Immunologics G100/rabbit polyclonal	1:4,000
L-glutamate	BSA–glutaraldehyde (L-glutamate) conjugate, rabbit	Signature Immunologics E100/rabbit polyclonal	1:32,000
L-glutamine	BSA–glutaraldehyde (L-glutamine) conjugate, rabbit	Signature Immunologics Q100/rabbit polyclonal	1:4,000
Taurine	BSA–glutaraldehyde (taurine) conjugate, rabbit	Signature Immunologics TT100/rabbit polyclonal	1:16,000

¹AGB, 1-amino-4-guanidobutane; GABA, γ -aminobutyric acid.

convergent and divergent ON input to several ganglion cell, GAC, and γ AC networks, thus constructing ON–OFF amacrine cells and ganglion cells and mediating within- and cross-channel inhibition. We show that both monad and dyad versions of axonal ribbons can involve single-ribbon or multiple-ribbon forms. Some rod bipolar cells possess axonal ribbons, but they are very close to their initial axon terminal branches, contact only A_I (A17) and A_{II} ACs, and do not supply the rod signals discovered in ipRGCs. Ultimately, analysis of axonal ribbons yields a refactoring of the mammalian IPL in which the OFF layer contains precisely multiplexed ON cone bipolar cell inputs.

MATERIALS AND METHODS

Tissue

Connectome volume RC1 was assembled from a light-adapted female Dutch belted rabbit (Oregon Rabbitry) after in vivo excitation mapping as described by Anderson et al. (2011a) in accordance with institutional animal care and use protocols of the University of Utah, the ARVO Statement for the Use of Animals in Ophthalmic and Visual Research, and the Policies on the Use of Animals and Humans in Neuroscience Research of the Society for Neuroscience.

Computational molecular phenotyping

Retinal neurons in RC1 were classified by computational molecular phenotyping (CMP) per Marc and Jones (2002) by using an array of small-molecule signatures (4-aminobutyrate [GABA], glycine, L-glutamate, L-glutamine, taurine, and the activity marker 1-amino-4-guanidobutane [AGB]). Briefly, the isolated rabbit eye was hemisected and immersion fixed overnight in 1% paraformaldehyde, 2.5% glutaraldehyde, 3% sucrose, 0.01% CaCl₂, in 0.1 M phosphate buffer, pH 7.4. Tissues were then dehydrated in graded methanols and acetone and embedded in epoxy resin. Tissues were then serial sectioned at 70–90 nm onto 12-spot Teflon-coated slides (Cel-Line; Fisher Scientific, Waltham, MA). Antibody exposure and silver intensification are described below under Small-molecular antibody characterization. Incubation of

TABLE 2.
IgG Competitive Sensitivities Computed From Inhibition Assays¹

Bis-conjugate	γ	G	E	Q	Ta
γ	0	8	5	7	6
G	6	0	5	7	6
E	4	9	0	5	6
Q	6	9	5	0	6
Ta	5	10	5	7	0

¹IgG competitive sensitivities computed from inhibition assays and expressed as log differential inhibition: $\log [C]/[T]$, where [C] and [T] are the concentrations of any conjugate (C) or the cognate target conjugate (T) required for 100% binding block. γ , GABA; G, glycine; E, glutamate; Q, glutamine; Ta, taurine.

all antibodies generated against small-molecular targets was performed overnight at room temperature, and visualization was with goat anti-rabbit secondary IgG coated with 1.4-nm gold (Amersham, Arlington Heights, IL) and silver intensified (Kalloniatis and Fletcher, 1993).

Small-molecular antibody characterization

Antihapten IgGs from Signature Immunologics (Salt Lake City, UT; Table 1) have been extensively characterized in prior publications (Marc et al., 1995; Marc, Marc, 1999a,b; Marc and Cameron, 2002; Marc and Jones, 2002). Each is an IgG isotype (determined by affinity chromatography and immunoblotting) produced in rabbit hosts immunized with glutaraldehyde–amino acid conjugates to bovine serum albumin (BSA) as described by Marc et al. (1995). Five analysis types were used to characterize the specificity and detectability of each anti-hapten IgG: 1) dependence on target molecule trapping; 2) immunodot assays against cognate small molecule–protein conjugates; 3) competition assays against free and bis-conjugates of small molecules (Table 2); 4) binding curves on quantitative artificial antigen stacks; and 5) cluster analysis (Marc et al., 1995).

RC1 assembly, analysis, and sharing

Bipolar cell networks in the ultrastructural rabbit retinal connectome RC1 (Anderson et al., 2011a) were

annotated with the Viking viewer (Anderson et al., 2011b) and explored via 3D rendering and graph visualization of connectivity (Anderson et al., 2011b). Small-molecule signals embedded in RC1 for CMP include 4-aminobutyrate, glycine, L-glutamate, L-glutamine, taurine, and the activity marker AGB. Combined with morphological reconstruction and network analysis, CMP permits robust cell classification (Anderson et al., 2011a). RC1 was acquired by ATEM at 2.18-nm resolution and assembled into a volume with the NCRTToolset (Anderson et al., 2009). Molecular-ultrastructural registrations were generated with ir-tweak (Anderson et al., 2009, 2011a,b). Three-dimensional renderings are built from disk annotations in Vikingplot (Anderson et al., 2011b), allowing rendering of surfaces and characterization of areas and volumes. All cells rendered in this article are publicly available as Google Colada *.dae files via the Connectome Viz application. These can be imported into 3D visualization tools such as Collada or Blender (www.blender.org). One defect in converting disk topologies to volumes for rendering of tapered processes sometimes led to somas or varicose neurites with vertically peaked shapes. These anomalies will be repaired in future code sets. Networks were visualized as directed multigraphs with Connectome Viz, and topologies were explored with Structure Viz (Anderson et al., 2011b). The RC1 data set and these associated analytical tools are publicly available at connectomes.uta.h.edu. Quantitative features of connections (numbers of synapses, axon dimensions, etc.) can be queried within these various tools and with Microsoft SQL.

Identification of IPL layers

The ON–OFF border of the IPL is not absolute, and we adopted a structural reference to define the transition between zones dominated by OFF and ON cone bipolar cells. In practice, the axial location of the ON–OFF border was set as the most proximal surface of the A_{II} AC lobule nearest a given bipolar cell. The OFF layer was defined as the region between the most distal GABA⁺ (γ^+) processes and the ON–OFF border. Similarly, the ON layer was defined as the region between the most proximal γ^+ processes and the ON–OFF border. For simplicity, we refer to these regions as the “ON” and “OFF” layers, corresponding to the older but less descriptive sublamina a and sublamina b, respectively. As in previous work, we define the amacrine cell layer–IPL border as level 0 and the ganglion cell layer–IPL border as level 100 (Marc, 1986).

Cell classification

All cells were classified using three criteria: molecular signatures, synaptic connectivity, and morphology. Bipolar cells were further subclassified according to their stratifications within the IPL, compared with the rabbit

bipolar cell classification scheme outlined by MacNeil et al. (2004). An itemization of the rules required for cell identity follows.

Rules for bipolar cells

Virtually all bipolar cells possess ribbon synapses. Their somas reside in the inner nuclear layer (INL), and they are glutamate positive. Glycine-positive (G^+) bipolar cells coupled to A_{II} AC arboreal dendrites via gap junctions and stratified in the proximal 60% of the IPL were classified as ON cone bipolar cells, with their precise level of stratification used to further refine their class memberships (CBb3, CBb3n, CBb3–4, CBb4, CBb5, CBb6, wide-field cone bipolar cell, and rod bipolar cell). Anderson et al. (2011a) showed that quantitative G^+ signatures are an absolute discriminator of bipolar cell::A_{II} AC coupling. Glycine-negative (G^-) bipolar cells that stratified in the distal 40% of the IPL and were both presynaptic and postsynaptic to A_{II} AC appendages were defined as OFF cone bipolar cells, with their precise level of stratification used to further refine their class (CBa1, CBa1w, CBa1–2, CBa1–2n). Bipolar cells with G^- signatures stratified in most proximal IPL, presynaptic to A_{II} AC arboreal dendrites, neither postsynaptic nor coupled to them, and presynaptic and postsynaptic to γ^+ A_I ACs were classified as rod bipolar cells. There are 104 rod bipolar cells in RC1. These independent classifiers are, collectively, errorless (Anderson et al., 2011a). There are instances in which CBa and CBb terminals (never rod bipolar cells) make synaptic contacts lacking classical synaptic ribbons. We call these bipolar cell conventional synapses, and they occur in terminals with numerous ribbons at other sites. One glutamate-positive bipolar cell class (CBa1w) is presynaptic and postsynaptic to A_{II} ACs but lacks ribbons and makes only bipolar cell conventional synapses. These cells are not discussed in this article, because they are not involved with the characterization of axonal synapses.

Rules for amacrine cells

Amacrine cells possessed conventional synapses only (not ribbon synapses), with somas residing in the INL, except for ON starburst amacrine cells, whose somas reside in the ganglion cell layer (GCL), and interstitial amacrine cells (IACs), whose somas reside mid-IPL. G and γ signals further refined their classification as GACs and γ ACs. Cells with moderate glycine signals, presynaptic lobular appendages in the OFF IPL, and coupled and postsynaptic arboreal dendrites in the ON IPL were defined as A_{II} ACs.

Rules for ganglion cells

Ganglion cells discussed in this paper were glutamate-positive, lacked presynaptic specializations, were never

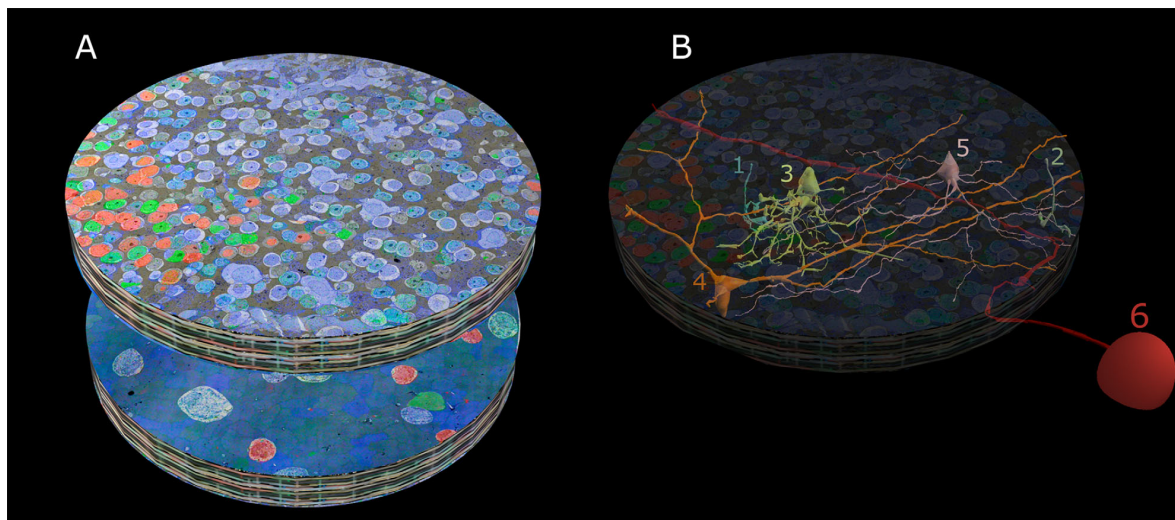


Figure 1. RC1 overview. **A:** The RC1 volume with its top section (001) beginning in mid-INL and ending in the GCL at section 371, shown in a mirror image below. RC1 is a short cylinder $\sim 250\ \mu\text{m}$ in diameter and $\sim 30\ \mu\text{m}$ high containing 341 TEM sections and 11 intercalated CMP sections. The cylinder is capped at top and bottom with 10-section CMP series, allowing molecular segmentation. TEM section 001 is a near-horizontal plane section through the INL visualized with GABA.glycine.glutamate \rightarrow red.green.blue transparency mapping and a dark gold alpha channel (ANDed taurine + glutamine channels) described by Anderson et al. (2011a). Similarly, TEM section 371 is a near-horizontal plane section through the GCL visualized with GABA.AGB.glutamate \rightarrow red.green.blue transparency mapping. **B:** Representative cells contained in RC1 are rendered in 3D onto the volume. Many complete copies of small cells exist (tens to hundreds), such as rod bipolar cells (cells 1, 2) and A_{II} ACs (cell 3). A few semicomplete copies (5–10) of medium-diameter cell classes have their somas and much of their arbors within RC1, but extend outside it, such as interstitial γ ACs (cell 4) and A_I amacrine cells (cell 5). Finally, RC1 contains many processes from partial cells: large cells such as wide-field amacrine cells or OFF α ganglion cells (cell 6) with somas outside the volume and often fully traversing it.

postsynaptic to rod bipolar cells, and had somas placed in the GCL or processes that traversed the entire volume. Based on cone bipolar cell input patterns, they were further classified as ON, OFF, or ON-OFF. Some classes were also γ^+ to differing extents (Marc and Jones, 2002) as a result of amacrine cell coupling.

Axonal ribbon synapses

Axonal ribbon synapses were defined by presynaptic and postsynaptic form in all cases, with the presynaptic ribbon itself surrounded by a halo or cluster of synaptic vesicles, a dense presynaptic membrane, complete glial withdrawal from the contact site, an evenly spaced synaptic cleft, and an unambiguous postsynaptic density on the target process. Synaptic clefts of synapses sectioned at oblique angles were often obscured but were recaptured via goniometric reimaging at higher resolution when necessary. Axonal ribbon synapses were defined as residing distal to the first branch point of each bipolar cell's primary axonal arborization. Although this criterion is formally arbitrary, it distinguishes pure axonal ribbons from those in the thin branches between terminal swellings in the axonal arbors.

Image preparation

As described in our prior articles on connectomics (Anderson et al., 2009), display transmission electron microscopic (TEM) images in this article were produced by remapping RC1 volume tiles to gamma 1.3. Optical and TEM overlays used the TEM gray-scale brightness combined with the hue, and saturation from the optical image as described by Anderson et al. (2011a). Three-dimensional versions and network maps of annotated cells were generated in Vikingplot and Viz applications (Anderson et al., 2011b).

RESULTS

The rabbit retinal connectome volume RC1 is a serial-section, 2-nm-resolution, 16.4-terabyte (TB) TEM image collection assembled into a cylindrical data volume $\sim 0.25\ \text{mm}$ wide and $\sim 0.025\ \text{mm}$ high spanning the mid-INL through the GCL (Fig. 1A), augmented by molecular channels capping and intercalated every 30 sections through it (Anderson et al., 2009, 2011a,b). The CMP channels include aspartate, glutamate, 4-aminobutyrate (GABA), glycine, glutamine, taurine, and AGB as a marker of light-driven activity. These channels permit robust classification of cells (Anderson et al., 2009, 2011a,b; Marc

TABLE 3.
Synapse Color Scheme: 3D Reconstructions

Synapse type	Color
Ribbon	Green
Conventional	Blue
Postsynaptic density	Red
Gap junction	Yellow
Adherens junction	White
Cistern contact	Gray

and Jones, 2002; Marc et al., 1995) and form an analytic statistic independent of morphological and network motif measures. The 0.25-mm-wide volume disc represents a mixture of sampling domains including complete, semi-complete, and partial architectures (Fig. 1B). The complete architectures include ~360 bipolar cells and ~50 narrow-field amacrine cells. The semicomplete architectures include ~40 bipolar cells, ~50 medium- to wide-field amacrine cells, and 15 ganglion cells with somas in the volume and dendrites extending beyond it. The partial architectures include large numbers (hundreds) of traversing amacrine cell and ganglion cell dendrites and axonal amacrine cell fields arising from somas outside the volume. This in no way invalidates use of partial architectures. Many of these traversing elements are still identifiable from their molecular signatures and corresponding network motifs. The size of the volume is limited by storage and time. The 2-nm resolution essential for mapping small synapses, and the gap junctions that provide diverse coupling topologies in retinal networks and serve as network identity signatures for specific neurons, required 16.5 TB of raw data and ~50 TB total which required 5 months to image. A volume containing complete wide-field amacrine cells would require many years of capture time to produce. Even so, the network motifs that emerge from deep analyses of partial elements such as crossing ganglion cell dendrites still accurately capture the native structure of the source cells, especially insofar as no evidence exists for (and much against) network anisotropy in individual ganglion cell and amacrine cell dendrites. Finally, the connectivity map of any volume is a compromise between intrinsic connections arising from cells completely inside the volume and extrinsic connections arising from cells outside the volume. For example, cortical connectome volumes contain far more extrinsic than intrinsic elements (Briggman and Bock, 2011). For the purposes of this article, we mined the axons of all bipolar cells for the presence of axonal ribbons and reconstructed the targets of these ribbons. Table 3 gives a legend for the color scheme used to represent synapse types in all 3D reconstructions displayed throughout this article. All cell identification numbers used here are identifiers that can be invoked in Viking, VikingPlot, and Viz

tools (Anderson et al., 2011a) to validate all of the ultrastructural features, network motifs, and statistics that we report here. RC1 is an open-source, open-access, open-data resource.

ON cone bipolar cell axonal ribbons throughout the OFF IPL form accessory ON pathways

ON cone bipolar cells make numerous axonal ribbon contacts throughout the OFF IPL: 175 of 398 (44%) bipolar cells in RC1 are ON cone bipolar cells. Thirty-four of these bipolar cells are semicomplete, with incomplete descending axons, so we cannot determine the frequency of axonal ribbons in this subset. Fifty-four of the remaining complete 141 ON cone bipolar cells possess axonal ribbons (Fig. 2). Thus 38% of the measurable ON cone bipolar cells make accessory ON axonal synapses. Three of these contain axonal ribbons only in the ON IPL; the remaining 51 of 141 bipolar cells (36%) contain one or more axonal ribbons in the OFF IPL. Most of these make multiple contacts through the OFF IPL, and, on average, each ON cone bipolar cell that makes axonal synapses will do so in three different instances. For clarity, we will use the MacNeil et al. (2004) rabbit bipolar cell morphological classification scheme to describe bipolar cells throughout this article. Briefly, the MacNeil et al. (2004) scheme abbreviates “cone bipolar” as “CB,” OFF laminae of the IPL as “a,” and ON laminae of the IPL as “b,” with numbers representing the specific IPL sublaminae within which bipolar cell axons primarily arborize. For instance, an OFF cone bipolar cell that primarily arborizes in sublamina 1 is referred to as “CBa1,” and an ON cone bipolar cell that primarily arborizes in sublamina 5 is referred to as “CBb5,” etc. Wide-field bipolar cells and rod bipolar cells are simply stated as such. Further cone bipolar cell subsets deemed as narrow and wide are additionally labeled with “n” or “w,” respectively, as in “CBb3n” or “CBa1w.” We introduce two newly discovered morphological bipolar cell classes, CBb5w and CBb6, which make axonal ribbons. Moreover, all major classes of ON cone bipolar cell (CBb3, CBb3n, CBb3–4, CBb4, CBb5, CBb5w, CBb6, wide-field cone bipolar cell) make axonal ribbons, five of which are highlighted throughout this article (Fig. 3). CBb5w cells costratify with CBb5 cells, yet they possess axonal arbor field diameters of ~40–55 μm vs. the 25–40- μm field diameters of most cone bipolar cells. CBb6s are nonwide-field bipolar cells that stratify alongside rod bipolar cells, more deeply than any other class of cone bipolar cell.

Previous studies indicated that the functional IPL stratification schemes require amendment to include an accessory ON layer at the most distal portion of IPL stratum 1

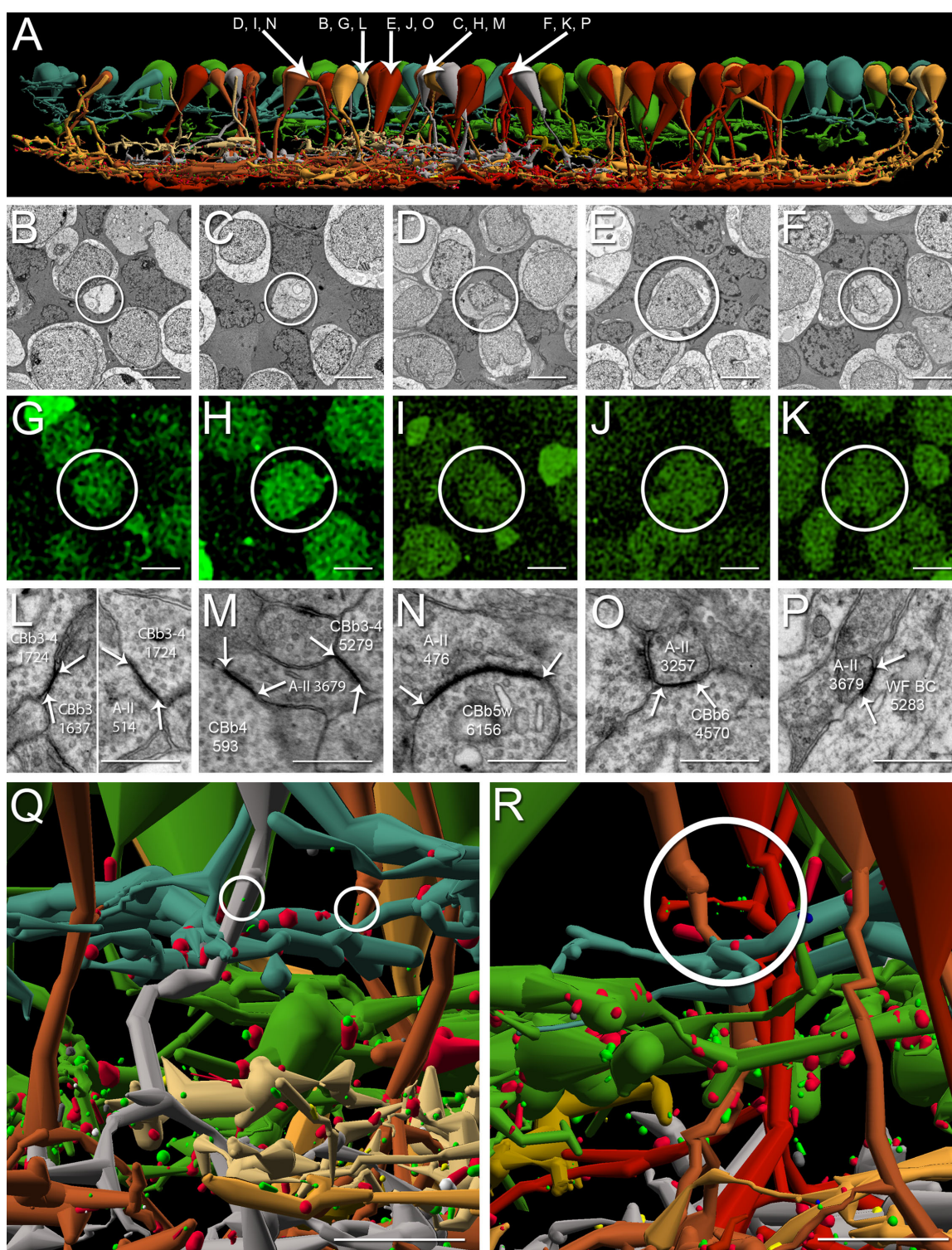


Figure 2

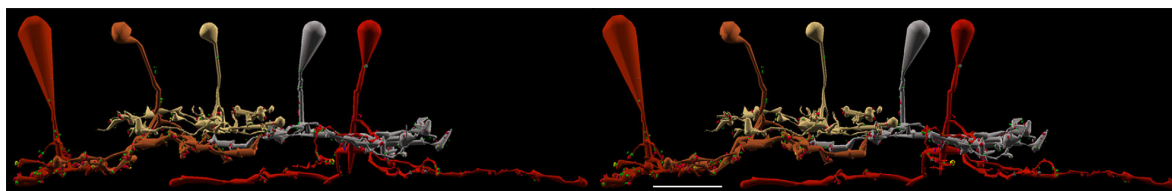


Figure 3. All major classes of ON cone bipolar cells possess axonal ribbons; stereogram. The five CBbs highlighted in Figure 2 are displayed in isolation for clarity. Varied numbers of axonal ribbons across CBb classes span the IPL. Cone bipolar cell color corresponds to depth of IPL stratification. Specific cone bipolar cell colors as follows: CBb3, tan; CBb4, silver; CBb5w, copper; CBb6, bright red (left); wide-field cone bipolar cell, deep red (right). Note the class-specific arborization thickness, pattern of varicosities, and axonal arbor diameters. Spatial relationships are preserved. Scale bar = 10 μ m.

and perhaps throughout the entire OFF IPL (Dumitrescu et al., 2009; Hoshi et al., 2009). Our data are consistent with mixed ON–OFF processing throughout levels 0–45% of the IPL, consistent with bipolar cell stratification patterns in nonmammalians.

Rod bipolar cell axonal ribbons do not provide accessory ON drive

In contrast to CBbs, 61 of 105 (58%) rod BCs also make bona fide axonal ribbon synapses (synapses in the axon above the primary branch point), but these are virtually all within the upper part of the ON IPL, with only a few breaking into the nominal OFF IPL (Fig. 4). Furthermore, virtually all of these (>90%) are contacts with identified A_I or A_{II} ACs. Every rabbit rod bipolar cell axon branches into two or three trunks as soon as it enters the ON IPL and immediately makes both pre- and postsynaptic specializations. The location of every axonal ribbon distal to the branch was mapped, and we found that 89% were exclusively in sublamina b, whereas 11% weakly breached the a/b border by an average of 600 nm. Over 90% of the traced targets of rod bipolar cell ribbons were verified as

processes of A_I or A_{II} ACs. Indeed, all the A_{II} AC processes were arboreal dendrites and never lobules.

CBb axonal ribbon frequency is approximately three times greater than that of rod axonal ribbons, and CBb axonal ribbon frequency (122 axonal ribbons) in sublamina a is approximately eight times greater than that of rod axonal ribbons (15 axonal ribbons), for fewer bipolar cells. Furthermore, the IPL ON–OFF border is not distinct but is rather a blend of CBa and CBb terminals. The distribution of CBb axonal ribbons represents a unique accessory pathway in the OFF channel, whereas the distribution of rod bipolar cell axonal ribbons reflects the targeting of normal ON pathway amacrine cells near the a/b border.

The upper 80% of the OFF IPL displays no rod bipolar cell axonal ribbons. We posited that this might be due to the heavy layer of Müller cell processes ensheathing the rod bipolar cells. This may be partially correct but clearly depends on the nature of the target. For example, arboreal dendrites of A_{II} ACs readily induce desheathing of rod bipolar cell axons, but lobular processes never do, leading to an obvious bias for forming axonal ribbons in the ON IPL. However, A_I ACs, which are both presynaptic and postsynaptic to rod bipolar cells in the ON IPL,

Figure 2. A subset of ON cone bipolar cells makes en passant and branched axonal ribbons. **A:** Vertically oriented renderings of 53 CBbs (neutral and warm colors) with axonal ribbons in the OFF IPL plotted against 48 CBas (cool colors). Cone bipolar cell color corresponds to depth of IPL stratification as follows: CBa1, sage; CBa2, green; CBb3, tan; CBb3–4, dark mustard; CBb4, silver; CBb5, mustard; CBb5w, copper; CBb6, bright red; wide-field cone bipolar cell, deep red. Arrows, somas of CBbs referenced in B–P. **B–K:** CBbs indicated in A are confirmed as glycine-positive (B–F, TEM of CBb somas; G–K, glycine-positive labeling of corresponding somas in B–F). **L–P:** TEM of gap junctions between CBbs indicated in A and A_{II} ACs. White arrows delineate gap junctions; A–II, A_{II} amacrine cell; WF BC, wide-field bipolar cell. **A,B,G,L:** CBb3 1637 rendering (A), TEM of soma (B), corresponding glycine-positive signature (G), and indirect A_{II} AC coupling via a gap junction with CBb3–4 1724 (L, left), which is coupled to A_{II} AC 514 (L, right). **A,C,H,M:** CBb4 593 rendering (A), TEM of soma (C), corresponding glycine-positive signature (H), and gap junction with A_{II} AC 3679 (M). **A,D,I,N:** CBb5w 6156 rendering (A), TEM of soma (D), corresponding glycine-positive signature (I), and gap junction with A_{II} AC 476 (N). **A,E,J,O:** CBb6 4570 rendering (A), TEM of soma (E), corresponding glycine-positive signature (J), and gap junction with A_{II} AC 3257 (O). **A,F,K,P:** Wide-field cone bipolar cell 5283 rendering (A), TEM of soma (F), corresponding glycine-positive signature (K), and gap junction with A_{II} AC 3679 (P). **Q:** CBb4 485 (silver) and CBb5w 180 (copper) form en passant axonal ribbon synapses (circles) among CBa1 and CBa2 arbors. **R:** Wide-field cone bipolar cell 16026 (red) forms branched axonal ribbon synapses (circle) among CBa1 and CBa2 arbors. Scale bars = 25 μ m in A; 5 μ m in B–K,Q,R; 0.5 μ m in L–P.

effectively induce desheathing in the OFF IPL and were presynaptic to rod bipolar cell axons (this network will be the subject of other papers) but were never postsynaptic. Thus, the formation of axonal ribbons is both site and function specific. The comparison of rod bipolar cell and ON cone bipolar cell ribbons shows that their roles are very different.

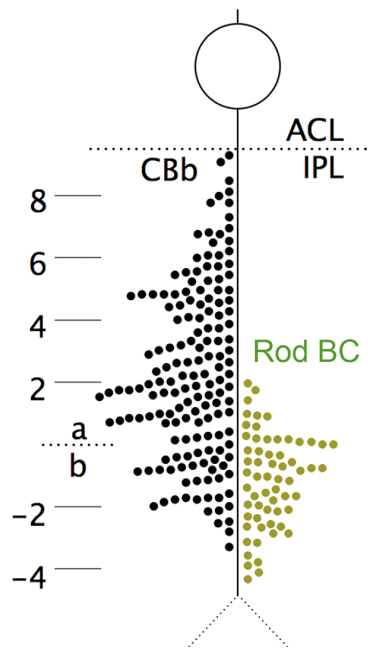


Figure 4. CBb vs. rod bipolar cell axonal ribbon depths. The distribution of 160 axonal ribbons in 54 CBbs and 63 ribbons in 63 of 104 rod bipolar cells in RC1. Ribbon positions are measured relative to the sublamina a/b border, defined as the proximal face of the nearest A_{II} amacrine cell lobule. CBb axonal ribbons are distributed throughout sublamina a. Rod bipolar cell axonal ribbons are excluded from 80% of sublamina a. ACL, amacrine cell layer; rod BC, rod bipolar cell.

Finally, although ipRGCs receive rod signals (Aggelopoulos and Meissl, 2000; Dacey et al., 2005; Wong et al., 2007), the network pathway for this transmission remains unclear. The primary and secondary scotopic pathways and rod bipolar cell axonal ribbon pathways have all been implicated, so we examined the relationship between rod bipolar cell axonal ribbons and M1 ipRGCs in the RC1 volume. We discovered that rod bipolar cell axonal ribbons are not cospatial with an M1 ipRGC dendrite present in the RC1 volume (Fig. 5), so this pathway cannot provide rod signals to M1 ipRGCs in the rabbit retina. Although ipRGC 12208's identity cannot be absolutely confirmed because there was no melanopsin immunolabeling in RC1, it monostратifies at the IPL/INL border, branches sparsely, accepts axonal ribbon input from every ON cone bipolar cell that it contacts (wide-field cone bipolar cell 6156 and wide-field cone bipolar cell 5283), and refuses input from two OFF cone bipolar cells (Fig. 4G,H). All of these features are consistent with M1-type ipRGCs (Dumitrescu et al., 2009; Graham et al., 2008; Hoshi et al., 2009). Henceforth, we shall simply refer to it as "ipRGC 12208."

Ganglion cell targets

We identified axonal ribbons from CBbs in the OFF IPL targeting bsdGCs, multistratified ganglion cells, ipRGCs, and other ON–OFF multistratified and OFF layer monostратified ganglion cell processes (Fig. 6). Unexpectedly, a chain of coupled ON cone bipolar cells provides axonal ribbon input to the bsdGC. Furthermore, multiple ON cone bipolar cell classes synaptically converge to common targets, and individual ON cone bipolar cells diverge to multiple targets, via axonal ribbons.

First, CBb4 3116 forms an axonal ribbon dyad onto bsdGC 15796 and a currently unidentified target (Fig. 6A,E). bsdGCs were identified in rabbit with dendrites that rise through the ON layer to stratify in the OFF IPL, where they receive CBb axonal ribbon input

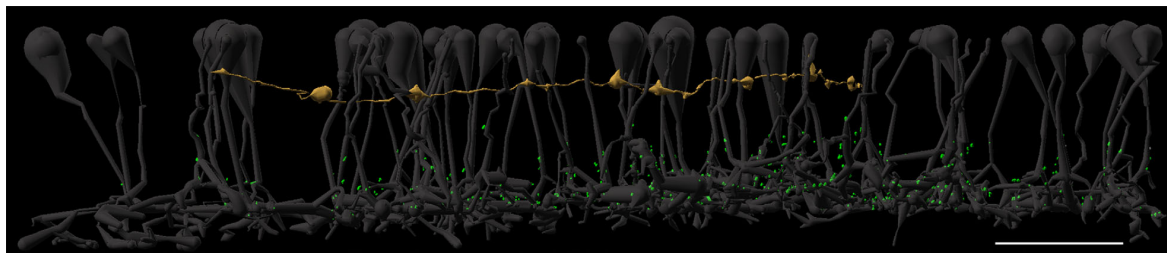


Figure 5. Rod bipolar cell axonal ribbons cannot drive M1 ipRGCs. All 63 rod bipolar cells (ghosts) with axonal ribbons in RC1 are displayed against ipRGC 12208 (sand). Note that all ribbon synapses (bright green dots), including the axonal ribbons, are too proximal in the IPL to form synapses with the ipRGC. Scale bar = 20 μ m.

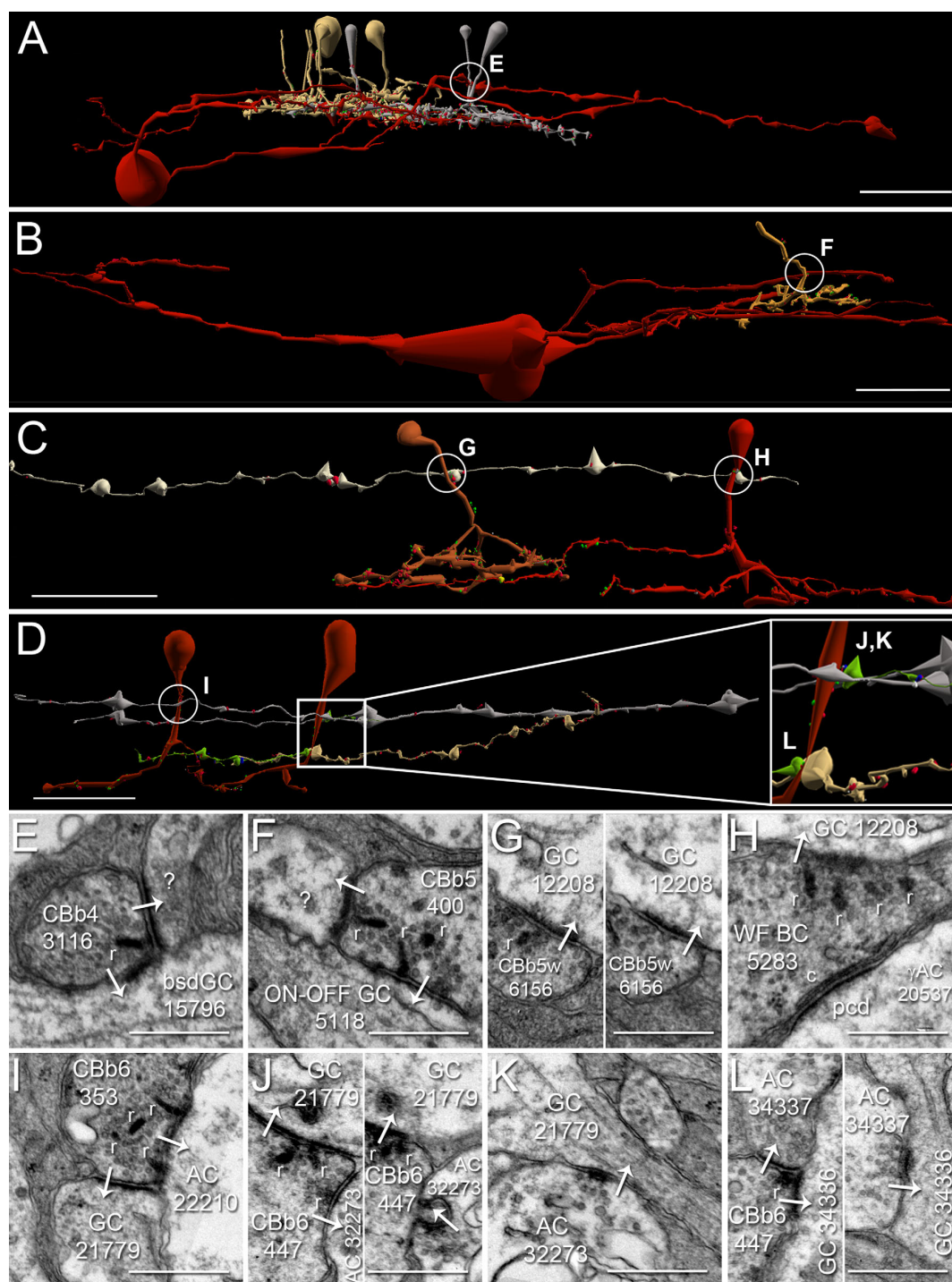


Figure 6

before re-entering the ON IPL (Hoshi et al., 2009). The bsdGCs may be the same as the G9 ganglion cell identified by Roska and Werblin (2003), with depolarizing responses to light blocked by L-APB and enhanced by

glycine and GABA receptor antagonists, and thus appear to be directly excited by ON cone bipolar cell input despite multistratification in both the ON and the OFF IPL. Note that the ganglion cell target process ascends to the

OFF sublaminae, where it receives the axonal ribbon input, then more distally returns to approximately the same IPL depth as the primary axonal arborization of the CBb4 that provides the axonal input. No OFF cone bipolar cell input to this ganglion cell has been found, despite abundant contact opportunities. Interestingly, CBb4 3116 participates in a chain of coupled CBbs across classes (CBb3 and CBb4). Moreover, none of these other CBbs, except for CBb4 3116, has been discovered to synapse onto bsdGC 15796 despite costratification of their primary axonal arbors with it. CBb4 3116 provides input only to bsdGC 15796 at the axonal ribbon location in the OFF IPL. Furthermore, the descending axon of CBb4 4569, one of the chain of coupled CBbs, passes within 0.25 μm of the axonal ribbon input to bsdGC 15796 by CBb4 3116 and does not form an axonal ribbon. These results are consistent with and extend those of Hoshi et al. (2009) by validating the selective input from CBb cells in the OFF layer.

Second, an axonal ribbon contact from CBb5 400 drives multistratified ganglion cell 5118. We cannot currently verify whether this ganglion cell is a bsdGC or an ON-OFF ganglion cell, because its OFF layer-stratifying processes exit the volume without descending to ON layers, and no OFF inputs have been discovered as yet. That said, ganglion cell 5118 appears morphologically distinct from bsdGC 15796, so it is likely of a different ganglion cell class.

Third, CBb5w 6156 and wide-field cone bipolar cell 5283 convergently drive M1 ipRGC 12208 with axonal ribbons, a single-ribbon monad and four-ribbon monad, respectively (Fig. 6C,G,H). This convergent input from two CBb classes presumably indicates fusion of different CBb response profiles to extend the functional range of the ipRGC. This is concrete evidence for convergent axonal

ribbon input from multiple bipolar cell classes onto ganglion cells.

Fourth, CBb6 447 and CBb6 353 converge axonal ribbon synapses onto OFF layer monostratified ganglion cell process 21779, and CBb6 447 diverges its output across the OFF and ON IPL via another axonal ribbon synapse in the ON layer to multistratified ganglion cell process 34336 (Fig. 6D,J–L). Both ganglion cell processes branch sparsely or not at all as they traverse nearly the entire width of the RC1 volume (257 μm) with no evidence of somata, indicating dendritic arbor radii of ≥ 250 μm and, thus, diameters ≥ 500 μm . Therefore, ganglion cell 21779 could belong to one of several classes of OFF layer-stratifying ganglion cells but is unlikely to be an M1 ipRGC for two reasons. First, it monostratifies closer to the primary branch points of CBb3s than expected for an ipRGC. Second, it receives ribbon input from a partial trace of an OFF cone bipolar cell axonal arbor (data not shown), which is inconsistent with M1 ipRGC electrophysiology. Ganglion cell 34336 could belong to any number of multistratified ganglion cell classes. This constitutes the first evidence that axonal ribbons in a single ON cone bipolar cell divergently drive targets in both the ON and the OFF IPL. All three of the axonal ribbons (across both CBb6s) form dyads onto a ganglion cell and amacrine cell targets, and both the amacrine cell targets of CBb6 447 conventionally synapse onto the ganglion cell target, thus forming CBb > amacrine cell \geq ON-OFF ganglion cell feed-forward motifs (Fig. 6I–L). Furthermore, amacrine cell 32273 provides feedback onto a finger-like projection from CBb 447 in addition to the feed-forward to ganglion cell 21779, thus regulating both presynaptic bipolar cell release and postsynaptic ganglion cell membrane potential (Fig. 6J, right). Combined, these results demonstrate that axonal ribbons from multiple CBb

Figure 6. Ganglion cell axonal ribbon targets. **A–D:** Renderings of five CBb classes forming axonal ribbons onto multiple ganglion cell classes; vertical orientation. Circles indicate location of synapses shown in **E–L**. **E–L:** TEM of synapses indicated in **A–D**. White arrows indicate synapse directionality. GC, ganglion cell; WF BC, wide-field bipolar cell; AC, amacrine cell; r, ribbons; c, cistern; pcd, postcisternal density. **A,E:** CBb4 3116 (left cell of the silver pair that intersects ganglion cell 15796 [red]) forms an axonal single-ribbon dyad with bsdGC 15796 and an unknown cell. CBb4 3116 participates in a chain of seven coupled CBb3s (tan) and CBb4s (silver). The bsdGC 15796 dendritic target of the axonal ribbon abruptly ascends to the OFF IPL, where it receives the input before returning to the ON IPL distally (far right in **A**). **B,F:** CBb5 400 (mustard) forms an axonal multiribbon dyad with ON-OFF ganglion cell 5118 (red) and an unknown cell. **C,G,H:** CBb5w 6156 (copper) and wide-field cone bipolar cell 5283 (red) converge an axonal single-ribbon monad and axonal multiribbon monad, respectively, onto ipRGC 12208 (off white). Note the omega figure at right in **G**. Wide-field cone bipolar cell 5283 forms an axonal cistern onto γ AC 20537 (not shown in **C**; see Fig. 8B,C) in the same plane of section as the four-ribbon axonal monad onto ipRGC 12208. **D,I–L:** CBb6 353 (red, left cell) and CBb6 447 (red, right cell) both form multiribbon axonal dyads (**I,J**) onto OFF-layer monostratified ganglion cell 21779 (silver) and another amacrine cell, amacrine cell 22210 (not shown in **D** for clarity; **I**) and amacrine cell 32273 (upper bright green cell in **D** inset, **J**), respectively. Amacrine cell 32273 creates both feedback (**J**, right) and feed-forward (**K**) inhibition motifs via conventional synapses onto CBb6 447 and ganglion cell 21779, respectively. CBb6 447 also forms a single-ribbon axonal dyad in the ON IPL onto multistratified ganglion cell process 34336 (beige in **D**, **L**, left) and amacrine cell 34337 (lower bright green cell in **D**, **L**, left). Amacrine cell 34337 forms a conventional synapse onto ganglion cell 34336 (**L**, right), thus completing a feed-forward inhibition motif. Scale bars = 25 μm in **A,B**; 20 μm in **C,D**; 0.5 μm in **E–L**.

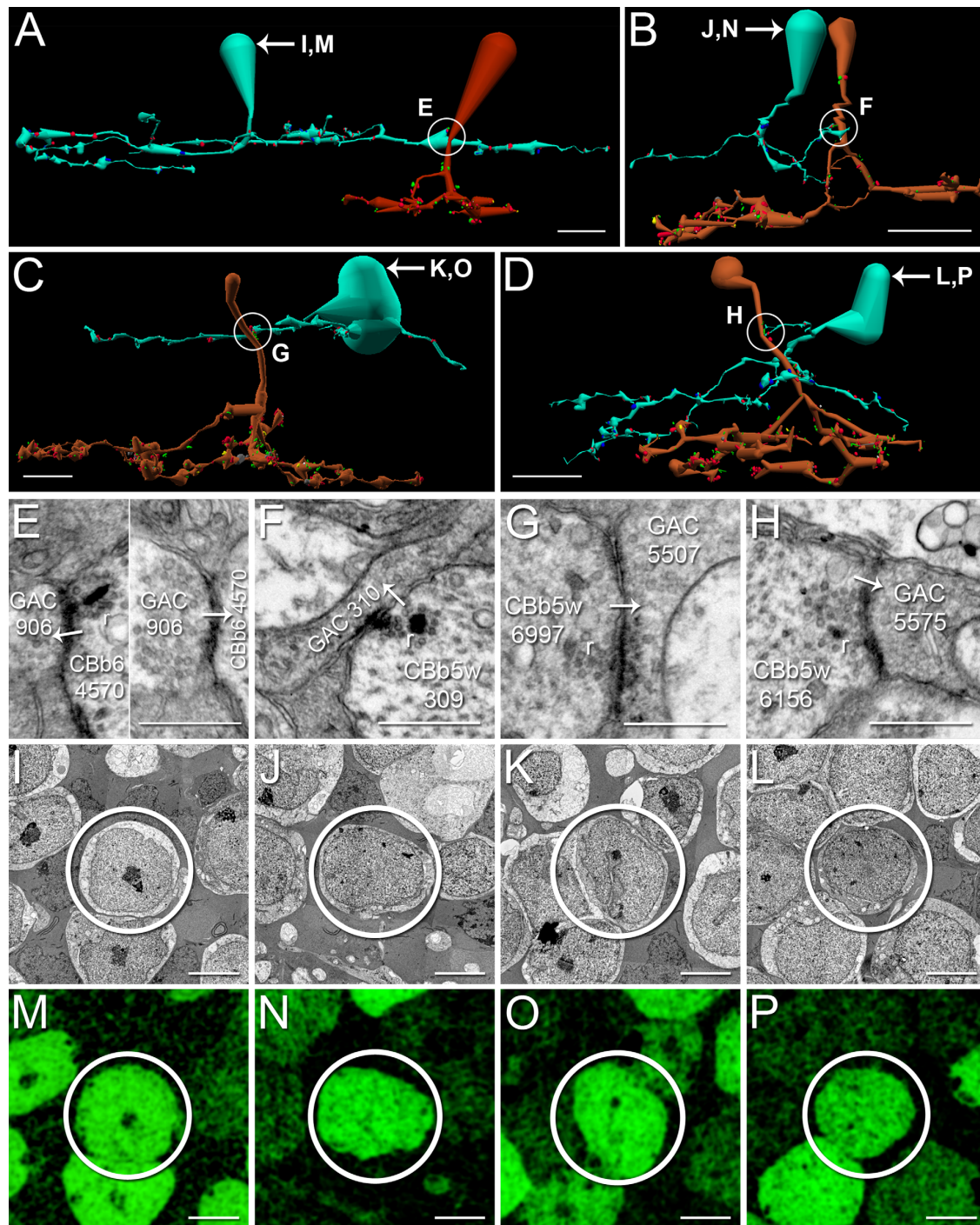


Figure 7. GAC axonal ribbon targets. A–D: Renderings of CBbs targeting both mono- and multistratified GACs with axonal ribbons; vertical orientation. Circles, locations of synapses shown in E–H; E–H: TEM of axonal synapses at locations indicated A–D. White arrows indicate synapse directionality. r, Ribbons. I–L: TEM of GAC somas. M–P: Glycine-positive signatures of the corresponding GAC somas in I–L. A,E: CBb6 4570 (red) forms a single-ribbon monadic reciprocal synapse with GAC 906 (patina). B,F: CBb5w 309 (copper) forms a single-ribbon monadic synapse onto GAC 310 (patina). C,G: CBb5w 6997 (copper) forms a single-ribbon axonal monad with GAC 5507. The ribbon is very light but possesses the characteristic halo of clear vesicles, and both pre- and postsynaptic densities are visible. D,H: CBb5w 6156 (copper) forms a single-ribbon axonal monad with GAC 5575 (patina). Scale bars = 10 μm in A–D; 0.5 μm in E–H; 5 μm in I–P.

classes convergently and divergently drive multiple classes of ganglion cells across OFF and ON sublayers and inject both ON excitation and ON inhibition to ON-OFF ganglion cells.

GAC targets

Axonal ribbons from at least two CBb classes target both mono- and multistratified GACs (Fig. 7). The first demonstrated reciprocal synapse at an axonal ribbon location appears between CBb6 4570 and monostratified GAC 906 (Fig. 7A,E), revealing axonal ribbons as sites of potential input as well as output. GAC 906 receives both ON and OFF inputs via monostratification in the overlapping region of ON-OFF processing in the mid-IPL described above. ON-OFF cells in the IPL are generally believed to be multistratified, yet this GAC, and ganglion cell 18693 described below, highlight ON-OFF comingling in the IPL as fundamental topology. This reinforces the facts that bipolar cells can multistratify to facilitate cross-channel communication and that they do not constrain their synaptic communication to discrete ON-OFF territories. GAC 5507 is currently a partial trace, so it is possibly multi- rather than monostratified (Fig. 7C,G). Multistratified GAC 5575 is particularly interesting, insofar as it extends a dendrite off its main trunk directly toward the descending axon of CBb5w 6156, where it receives axonal ribbon input (Fig. 7D,H). GAC 5575 divergently drives both ON cone bipolar cell \geq ON ganglion cell (bsdGC) and ON cone bipolar cell \geq ON-OFF ganglion cell inhibition, as described below. The combination of mono- and multistratified GAC targets suggests differential sign-inverting distribution of the CBb glutamatergic drive, but that will be explored in separate studies.

γ AC targets mediate within- and cross-channel inhibition

Three classes of ON cone bipolar cell were discovered to form γ AC-mediated within-channel (Fig. 8A) and cross-channel (Fig. 8B,C) inhibitory motifs with axonal ribbons. First, CBb5 5562 drives multistratified γ AC 5294 with an axonal ribbon (Fig. 8A,D,F). γ AC 5294 forms a conventional synapse onto the primary telodendria of CBb5 5645 (Fig. 8A inset, G), completing a within-channel inhibition motif. This within-channel inhibition is consistent with formation of the inhibitory surround of a center-surround receptive field for CBb5 5645, yet this is the first report of such surround inhibition arising from axonal ribbon drive. Second, CBb6 5536 divergently drives a pair of amacrine cells, one of which is γ^+ (Fig. 8E), at a branched axonal ribbon dyad site (Fig. 8B,C,H). Target amacrine cell 20537 is the γ AC dendrite, and it spans most of the width of the RC1 volume without attachment to its soma,

indicating a dendritic arbor radius of $\geq 250 \mu\text{m}$ and therefore a dendritic arbor diameter of $\geq 500 \mu\text{m}$. Thus γ AC 20537 is a wide-field γ AC. Target amacrine cell 19571 does not cross an immunolabeled section of the RC1 volume and cannot be confirmed as γ^+ , but it is glycine negative (data not shown) and possesses the characteristic light cytoplasm (clear varicosities) of γ ACs. Furthermore, the two amacrine cell targets form a nested feedback architecture onto CBb6 5536 (Fig. 8H, right), a γ AC network motif previously demonstrated in teleosts (Marc and Liu, 2000). Wide-field γ AC 20537 also receives branched axonal ribbons from wide-field cone bipolar cell 16026 (Fig. 8B,C, left inset, and I), which, combined with input from CBb6 5536, forms a CBb $>$ γ AC convergent motif. The second amacrine cell target of the divergence from the CBb6 5536 branched axonal ribbon creates a CBb $>$ γ AC \geq CBa crossover inhibition motif (Fig. 8B,C, right inset, and J).

Axonal cisterns appear in accessory ON networks

Axonal cisterns, reported by Anderson et al. (2011a), are characterized by a cistern adjacent to the plasma membrane of the nominal presynaptic cell, desheathed glia, an evenly spaced cleft similar to a synaptic cleft, and a definitive postcisternal density (PCD) indistinguishable from classic postsynaptic densities. As an example, some targets collect from multiple cisterns. In addition to its axonal ribbon input, γ AC 20537 contacts axonal cisterns from CBb5 176 and wide-field cone bipolar cell 5283 (Figs. 5H, 8B,K). The convergent axonal ribbon input to ipRGC 12208 described previously is linked to this γ AC axonal ribbon network via the axonal cistern and axonal ribbons in the same plane of section by wide-field cone bipolar cell 5283. Taken together, this partial network of axonal ribbons and cisterns illuminates the complexity of axonal communication. The simultaneous divergence and convergence illustrated by the branched axonal ribbon dyad and monad from CBb6 5536 and wide-field cone bipolar cell 16026, respectively, spotlight the efficient design inherent in these networks.

Divergent ON-OFF GAC inhibition to CBbs and ON-OFF ganglion cells

We explored identified GAC axonal ribbon targets as possible crossover candidates. Axonal ribbon-driven GACs can distribute ON-OFF inhibition to both CBbs and ON-OFF ganglion cells (Fig. 9). Specifically, the following network motifs exist: CBa $>$ ON-OFF GAC \geq CBb, CBa $>$ ON-OFF GAC \geq ON-OFF ganglion cell, and CBb $>$ ON-OFF GAC \geq ON-OFF ganglion cell, all three of which constitute ON-OFF cross-inhibition.

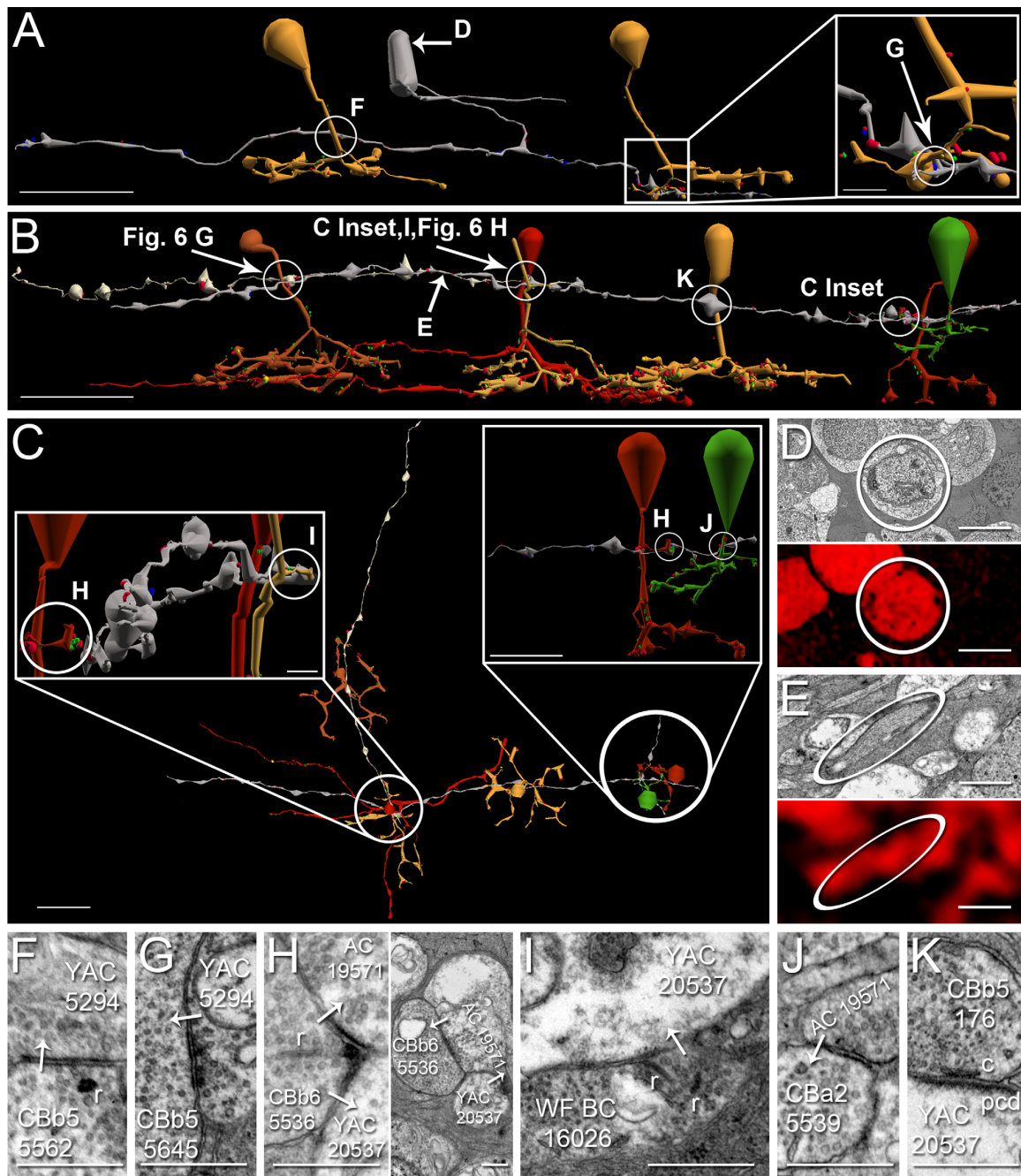


Figure 8

First, CBa2 424 and CBa2w 478 (a new CBa class discovered in RC1) drive monostratified GAC 906 with ribbon synapses (Fig. 9A,E,F). GAC 906 forms a conventional synapse onto CBb6 4570, reciprocal to an axonal ribbon (Figs. 7A,E 9A), thus bestowing ON-OFF properties to GAC 906 and constructing a CBa > monostratified

ON-OFF GAC \geq CBb crossover inhibition motif. ON-OFF GAC 906 also synaptically diverges this ON-OFF inhibition to monostratified ON-OFF ganglion cell 18693 (Fig. 9B,G). This is the first example of one GAC divergently distributing ON-OFF inhibition to both CBb and ON-OFF ganglion cell targets.

Next, CBb5w 6156 forms axonal ribbon synapses onto multistratified GAC 5575 (Figs. 7D,H,9B), and GAC 906 and GAC 5575 cross-inhibit each other (data not shown). GAC 906 therefore injects its ON-OFF properties to GAC 5575. Some ON-OFF amacrine cells are known to receive ON-OFF inhibition (Chen et al., 2011), and we add that the excitatory drive for this can arise from axonal ribbons. Each of the above-mentioned ON-OFF GACs makes conventional synapses onto mid-IPL monostratified ON-OFF ganglion cell 18693 (Fig. 9B,G-I), forming parallel CBb > ON-OFF GAC \geq ON-OFF ganglion cell motifs via two morphologically distinct GAC classes, thus blurring classical ideas of structure-function relationships. Clearly, the relationships are complex. The OFF input to GAC 906 from the two CBas further constructs a CBa > ON-OFF GAC \geq ON-OFF ganglion cell motif. Examples of GAC-mediated crossover inhibition motifs via axonal ribbons from ON to pure OFF targets remain to be discovered in RC1.

Divergent ON-OFF GAC inhibition to ON-OFF ganglion cells and bsdGCs

bsdGCs obtain ON polarity response properties via direct synaptic drive from CBbs, some of which arises from axonal ribbons (Hoshi et al., 2009; Roska and Werblin, 2003). Here we report that axonal ribbons also drive ON-OFF inhibition to bsdGCs via one branch of a divergent inhibitory pathway. ON-OFF GAC 5575, introduced above, not only mediates CBb > ON-OFF GAC \geq ON-OFF ganglion cell inhibition it also synaptically diverges its signals to bsdGC 15796 (Fig. 9B-D,H-J). This constitutes the first reported evidence that a single nar-

row-field multistratified GAC can disperse sign-inverted axonal ribbon excitatory signals to both ON-OFF ganglion cells and ON ganglion cells (bsdGCs) and emphasizes the inherently multiplexed nature of GACs.

ON cone bipolar cell axon tangency without axonal ribbon synapses

Thirty-eight percent of CBbs in RC1 make axonal ribbons, which raises the question of why the other 62% do not. This requires some new terminology. Most neurites in the retina are directly apposed to those of other neurons without forming any specialization such as a synapse, gap junction, or adherens junction (Anderson et al., 2011a). We refer to such neurite pairs as “tangent” processes. In some cases, a single descending axon simply bypasses a cell to which it is tangent without forming an axonal ribbon (Fig. 10A,C). More intriguing, two ON cone bipolar cell axons may be tangent to the same cell, with differential connectivity to it. For example, CBb4 3116 forms an axonal ribbon dyad onto a bsdGC 15796 and an unknown target, and CBb4 4569 is tangent to the same unknown process, without forming an axonal ribbon synapse (Fig. 10B,D). In the first case, the potential but unconsummated target is an OFF layer monostratified ganglion cell that may be a pure OFF ganglion cell, as we have identified only OFF cone bipolar cell input to this ganglion cell. Thus it may not be an appropriate target. In the second case, three interesting points arise: 1) the CBb without axonal ribbons in Figure 10 does not make *any* axonal ribbons, 2) the CBbs are of the same class (CBb4), and 3) the CBbs are coupled by gap junctions and therefore share signaling attributes. One possibility

Figure 8. γ AC axonal ribbon targets and axonal cisterns. **A–C:** Renderings of axonal-ribbon driven γ ACs mediating within- and cross-channel, divergent and convergent, inhibitory networks, vertical orientation (A,B), horizontal orientation (C). Arrows, locations of γ^+ signatures shown in D,E; circles, locations of synapses shown in F–K. **D,E:** TEM of γ ACs in A–C with corresponding γ^+ signatures. **F–K:** TEM of synapses indicated in A–C. White arrows indicate synapse directionality. AC, amacrine cell; WF BC, wide-field bipolar cell; r, ribbons; c, cistern; pcd, postcisternal density. **A:** CBb5 5562 (mustard, left) forms an axonal single ribbon monad (F) onto multistratified γ AC 5294 (silver). γ AC 5294 forms a conventional synapse (A inset, G) onto CBb5 5645 (mustard, right), thus completing an axonal ribbon-mediated within-channel inhibition motif. 5294's soma is γ^+ (D). **B:** A chain of five CBbs converge and diverge axonal ribbon and cistern contacts onto common γ AC and ganglion cell targets; vertical orientation. CBb6 5536 (red, right) provides divergent input to amacrine cell 19571 processes (silver) and wide-field γ AC 20537 (silver) with an axonal ribbon dyad (H) at locations indicated in C, insets. Wide-field γ AC 20537 is γ^+ (E). Amacrine cell 19571 cannot be confirmed as γ^+ but is glycine negative and participates in nested feedback with γ AC 20537 (H, right). CBb5 176 (mustard) and wide-field cone bipolar cell 5283 (deep red, center) converge axonal cistern contacts onto γ AC 20537 (K, Fig. 6H). In the same plane of section, wide-field cone bipolar cell 5283 drives ipRGC 12208 with a four-ribbon axonal monad (Fig. 6H). This ipRGC additionally receives convergent axonal ribbon input (Fig. 6G) from CBb5w 6156 (copper). **C:** Horizontal view of B. **Left inset:** Rotated and zoomed-in vertical view of the circled area in the main panel (some cells removed for clarity). CBb6 5536 (red, left) and wide-field cone bipolar cell 16026 (sand) provide convergent, branched axonal ribbon input to γ AC 20537 (H left). This view looks down the length of γ AC 20537 (silver) between wide-field cone bipolar cell 16026 in the right foreground and CBb6 5536 in the left background. Wide-field cone bipolar cell 5283 (red, right) can be seen close to wide-field cone bipolar cell 16026. **Right inset:** Rotated and zoomed-in vertical view of CBb > γ AC \geq CBa crossover inhibition. CBb6 5536 (red) provides a branched axonal ribbon dyad (H left) onto amacrine cell 19571 (silver). Amacrine cell 19571 forms a conventional synapse (J) onto CBa2 5539 (green) nearby, thus completing the crossover inhibition motif. Scale bars = 20 μ m in A–C; 5 μ m in D, right inset; 0.5 μ m in E–K; 2.5 μ m in left inset.

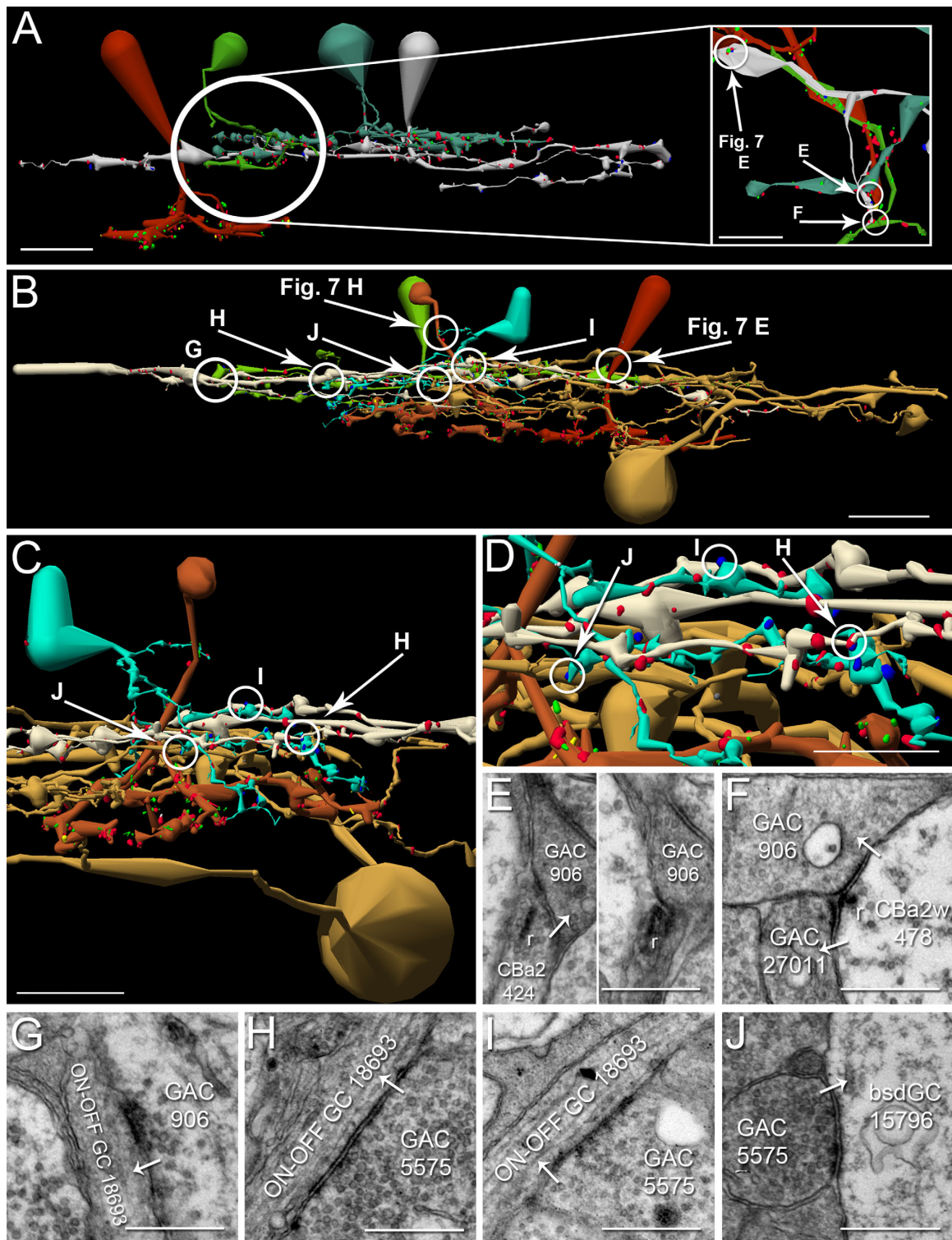


Figure 9

for the differential connectivity is that ON cone bipolar cell coupling overcomes the need for axonal ribbon input from both CBbs. That said, coupled CBbs do drive common targets from their telodendria, but never at the same locus. This topic will be addressed in future studies.

DISCUSSION

The analysis of RC1 and noncanonical ON cone bipolar cell axonal ribbon synapses in the OFF layer exposes new organizational concepts for the retina and leads to a refactoring of the IPL. We first address the existence of mixed signaling strata and new network access schemas, the distinction between simple tangency and functional contact, and the importance of joint distributions for interpreting synaptic statistics. Then we review key signaling features of specific targets of axonal ribbons. Because bipolar cell nomenclatures differ across species and we will now be discussing many of them, and because all cone bipolar cell classes in rabbit make axonal ribbons, we periodically depart from the McNeil et al. (2004) rabbit scheme for the discussion and simply refer to cone bipolar cells as ON cone bipolar cells and OFF cone bipolar cells.

First, why do ON cone bipolar cells target the OFF layer of IPL at all? The answer is partially evolutionary: the OFF layer of the IPL has been a mixed ON–OFF stratum throughout vertebrate descent. Every nonmammalian vertebrate class harbors multistratified ON bipolar cells (Kolb, 1982; Pang et al., 2004; Ramón y Cajal, 1892; Scholes, 1975; Scholes and Morris, 1973; Sherry and Yazulla, 1993; Wong and Dowling, 2005), and their discovery in the mammalian retina demonstrates that no evolutionary mechanism has ever “purified” the OFF

layer. More concretely, mixed strata reflect important network access properties. Axonal ribbons provide ON inputs to unique monostratified cells such as TH1 axonal cells and M1 ipRGCs (Dumitrescu et al., 2009; Hoshi et al., 2009) that send their dendrites to the most distal layer of the IPL. This is an incomplete explanation, because the very same ON cone bipolar cells also have outputs in the ON layer. The question should be reframed in future work: why do the target ON cells invade the OFF layer at all? We have preliminary data to show that, in addition to ON inputs, these cells seek inputs from CBa1-driven OFF γ ACs accessible only in the OFF layer. Ultimately, there is no unique distal ON stratum in the IPL. Indeed, the entire OFF layer is a stack of mixed ON–OFF strata with cone bipolar cell axonal ribbons distributed throughout (Figs. 2–4). We propose that ON signals in the OFF layer provide unique network opportunities for cross-over signaling and loci for mixing ON excitation with polarity-matched OFF inhibition.

Analysis of axonal ribbon sites reveals that specific rules control their incidence, although we clearly have a poor idea of the molecular mechanisms. ON cone bipolar cell axons are sheathed by three facing Müller cells throughout their transit of the OFF layer, except at sites of potential target contact, where the Müller cells are parted by unknown mechanisms. As described by Anderson et al. (2011a) and this manuscript, many neural processes are apposed without intervening glia but never make synapses, gap junctions, or even adherens junctions. As noted above, we refer to such lack of functional contact as “tangency.” Many processes somehow induce unsheathing of Müller cells around CBb cells in the OFF layer yet remain simply tangent. Another important point is that ribbon synapses, whether in the axon or in the

Figure 9. Novel network topologies construct an ON–OFF GAC and underlie glycine-mediated within- and cross-channel inhibition. **A–D:** Vertically oriented renderings of ON–OFF GAC construction, $\text{CBa} > \text{GAC} \geq \text{CBb}$ crossover inhibition (A), and $\text{CBb} > \text{GAC} \geq$ ganglion cell within- and crosschannel (crossover) inhibition motifs (B–D). Circles, location of synapses shown in E–J. **E–J:** TEM of synapses indicated by circles in A–D. White arrows indicate synapse directionality; GC, ganglion cell. **A,E,F:** Axonal ribbon topologies employed for construction of a *monostratified* ON–OFF GAC and $\text{CBa} > \text{GAC} \geq \text{CBb}$ crossover inhibition motifs. **Inset:** Rotated and zoomed-in horizontal view of CBa2 424 (green), CBa2 478 (sage), GAC 906 (silver), and CBb6 4570 (red). CBa2 424 and CBa2 478 converge a single-ribbon monad and single ribbon dyad onto GAC 906 (E–F). GAC 906 forms a conventional synapse onto CBb6 4570 (red), reciprocal to an axonal ribbon (Fig. 7A,E). **B,G–J:** Parallel $\text{CBb} > \text{GAC} \geq$ ON–OFF ganglion cell cross-channel inhibition and divergent within-channel ($\text{CBb} > \text{GAC} \geq \text{bsdGC}$) and cross-channel ($\text{CBb} > \text{GAC} \geq \text{ON–OFF ganglion cell}$) inhibition. CBb6 4570 (red) drives GAC 906 (green) at the axonal synapse described for A. GAC 906 forms a conventional synapse (G) onto monostratified ON–OFF ganglion cell 18693 (off-white). CBb5w 6156 (copper) drives narrow-field multistratified GAC 5575 (patina) with an axonal ribbon (Fig. 7H). GAC 5575 forms conventional synapses onto monostratified ON–OFF ganglion cell 18693 at two locations (H,I). These two synaptic chains thus form parallel $\text{CBb} > \text{GAC} \geq \text{ON–OFF ganglion cell}$ motifs that converge onto the same ganglion cell target. GAC 5575 also forms a conventional synapse (J) onto bsdGC 15796 (sand), thereby creating divergent inhibitory motifs driven by CBb5w 6156 to two distinct classes of ganglion cell. **C,H–J:** Rotated, zoomed-in, and isolated divergent inhibition shown in B. Multistratified, narrow-field GAC 5575 (patina) receives axonal ribbon input from CBb5w 6156 (copper) at an OFF-layer branch (Fig. 7D,H not circled for anatomical clarity) and forms conventional synapses (H–J) with ganglion cell 18693 (off-white) and bsdGC 15796 (sand). **D,H–J:** Zoom-in of GAC 5575 divergent inhibition in B,C for anatomical clarity and detail, better appreciation of network topologies, and synapse locations. Scale bars = 10 μm in A,D; 5 μm in inset; 20 μm in B,C; 0.5 μm in E–J.

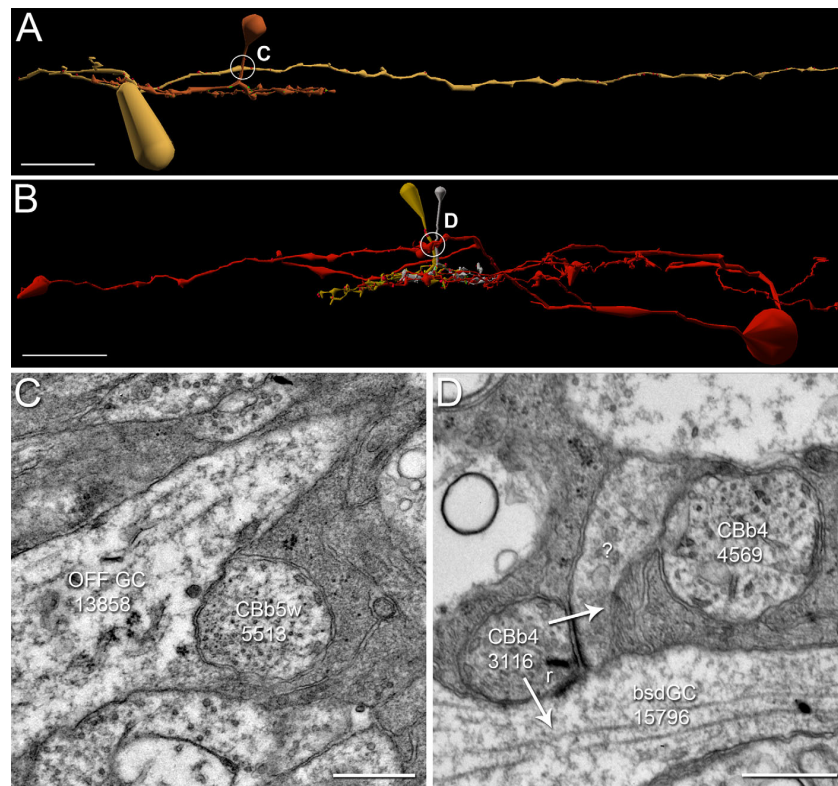


Figure 10. CBb axon tangency to potential targets without axonal ribbon synapses. **A,B:** Renderings of CBbs with contact, but not synapses onto ganglion cells; vertical orientation. Circles, locations of synapses shown in **C,D**. **C,D:** TEM of synapses indicated by circles in **A,B**. White arrows indicate synapse directionality; GC, ganglion cell. **A,C:** CBb3 5513's (copper) axon is tangent (adjacent with no intervening muller glia) to OFF ganglion cell 13858 (sand), yet does not form a synapse. **B,D:** CBb4 3116 (silver) forms an axonal ribbon dyad onto bsdGC 15796 (**D**; see also Fig. 6A,E) and an unknown target (**D**), whereas CBb4 4569 (dark mustard) does not form an axonal ribbon onto the same unknown target despite being tangent to it. Incidentally, CBb4 3116 and CBb4 4569 are gap junctionally coupled (data not shown). Scale bars = 20 μ m in **A,B**; 0.5 μ m in **C,D**.

axon terminal, never appear at the membrane without an associated postsynaptic density. This suggests that complete synaptic contacts are induced by the target or source–target interactions but that unsheathing to expose the source seems to be under control of the target.

Finally, not all ON cone bipolar cells in a given class form axonal synapses, but members of all classes do form OFF layer axonal synapses. With a very strict criterion, 38% of all identified ON cone bipolar cells in RC1 engage the OFF IPL with axonal ribbon synapses. Our analysis of sources and targets for these and other synaptic pairings suggests that the retina routinely invokes such partial motifs. Such sampling schemes conflict with our traditional expectations and methods of tabulating synaptic contacts (e.g., calculating the percentage of outputs onto a target). That approach to network analysis would lead us to ask the following: if most ON cone bipolar cells do not form axonal synapses, how can we argue that they are functional and not some statistical anomaly?

We can approach this problem via graph theory, with cells represented as vertices and synaptic connections represented as edges. Every vertex in a directed graph represents a point of signal transfer between a source and target. In a multidigraph like the retina (Marc et al., 2012), each vertex represents the source or target for multiple edges, and, given that the copy numbers for each class of vertex (i.e., each *ultimate* cell class; Marc and Jones, 2002) varies, as do their coverages and Hausdorff dimensions, one cannot optimize a complex biological system to give smooth statistics or provide 100% source contacts for all cells. Figure 11 provides a geometric proof of this. The white dots in Figure 11 represent the projection of 15 ON cone bipolar cell axons through a sampling plane of the IPL. In Figure 11A, a set of cells from a single class (with individual cells in different colors) with a high coverage contacts every cone bipolar cell axon. Indeed, the overlap of individual cells leads to multiple edges. The outflow efficiency *appears* to be 100%,

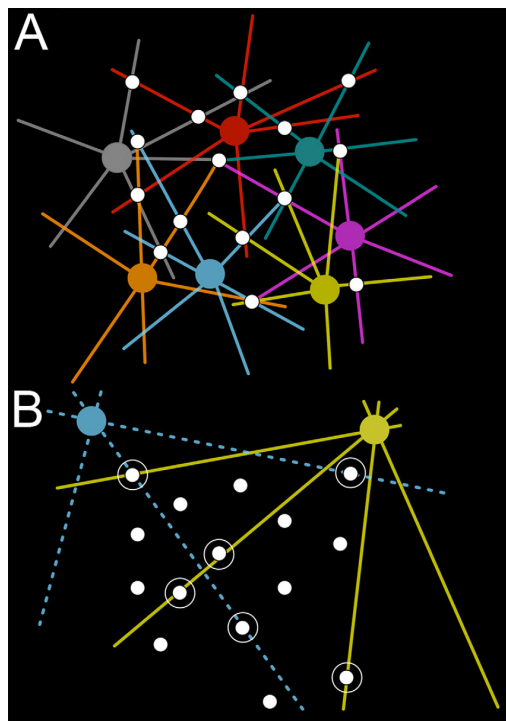


Figure 11. Explanation of the interaction between sparse network topologies and joint distributions. **A:** An array of bipolar cell axons (white) traverses the image plane of the retina. In the top field, a cell class with high coverage is shown in different colors for every instance of the class. Each bipolar cell axon is contacted several times for an average contact of 2.4. **B:** Two different classes of ganglion cells (yellow, blue) form part of their tiling by sampling from the bipolar cell array. Most bipolar cells are missed, for an average outflow contact of 0.375, which is meaningless. Six circled bipolar cells are contacted by the ganglion cells (none twice), and the ganglion cells are errorless in contacting encountered bipolar cells. Because ganglion cells are not space-filling cells, further inputs would be superfluous.

with a mean contact number of 2.67 ± 0.7 (standard deviation), but it is important to grasp that these are meaningless metrics, especially the variance. The only metric that matters is the efficiency of target sampling, which is also 100%. This becomes clearer in Figure 11B, in which two different, sparse cell classes send dendrites through the axonal field. Only six of 15 axons are hit, for an output efficiency of 40%. Indeed, the output efficiency is even lower for each class, yet, from the perspective of the targets, the two cells make synapses with 100% of the axons that they encounter. This is critical for cells with low coverages, such as ganglion cells. Their target sampling is perfect. Not all axons are hit, because there is an oversupply of sources. The target does not “know” that there are excess source axons, because they are not

needed. Thus the partial incidence of axonal synapses in ON cone bipolar cell axons reflects the spatial needs of the targets, not the sources. It does not represent any imprecision, QED. The key descriptor for such networks is the joint density distribution of source and target, expressed as a metric of signal transfer sites per unit area or volume of neural space.

Two ON cone bipolar cell classes converge onto ipRGCs

The putative ipRGC identified in RC1 receives axonal ribbon input from every ON cone bipolar cell that it encounters, wide-field cone bipolar cell 5283 and CBb5w 6156. It further refuses input from two OFF cone bipolar cells to which it is tangent (data not shown). Neural structure–function correspondence is widely agreed upon, and every tested class of bipolar cell identified based on unique morphology has thus far proved to possess unique physiological response properties (Masland, 2001). Thus wide-field cone bipolar cell 5283 and CBb5w 6156 contribute their presumably differential response properties via sign-conserving synapses to the ipRGC, thereby increasing the complexity or range of the ipRGC responses. This could represent convergence of different spectral sensitivities and/or flux range fractionation.

Coupled bipolar cell input to bsdGCs

bsdGC 15796 is one target of an axonal ribbon dyad from CBb4 3116 (Fig. 6A), which belongs to a cluster of seven coupled ON cone bipolar cells that likely represent a patch in a larger sheet of coupled cone bipolar cells, similar to the coupled clusters of ON cone bipolar cells discovered in teleosts (Umino et al., 1994). It is striking that none of the other members of the coupled chain provides input to the bsdGC, despite a second axon from CBb4 4569 very close to the axonal ribbon input by CBb4 3116 (Figs. 6A, 10B,D) and costratification of ON cone bipolar cell primary axonal arbors with ON layer bsdGC arbors. Again, this reflects the concept of joint distributions in which a limited bsdGC target architecture samples inputs from an array of excess sources. This would be especially true when sampling from coupled arrays, because a single sampled input would provide some weighted mean output from a patch. Teleost coupled bipolar cells appear to receive variable input from cones, which introduces noise into the system, and modeling coupled bipolar cells as hexagonal arrays of isopotential units indicates that coupling increases the input signal-to-noise ratio without significantly sacrificing resolution (Umino et al., 1994). bsdGCs receive most of their ribbon input in the ON layer (Hoshi et al., 2009), and the need for axonal ribbon input remains a mystery.

As noted above, it is likely that the primary function of OFF stratification in nominal ON cells is accessing OFF amacrine cell inputs.

γ AC targets, GAC targets, and crossover inhibition

Physiological analyses show that ON and OFF channels cross-inhibit each other via glycinergic synapses at every tier of the IPL (Chen et al., 2011; Molnar et al., 2009; Roska and Werblin, 2003; Werblin, 2010). Functional reasons for this include possible restoration of linearity to rectified currents driven by AMPA and NMDA receptors, expanding photopic dynamic range into the scotopic domain, luminance-contrast distinction, better impedance matching in postsynaptic neurons, OFF cone bipolar cell gain, and high-frequency-response increase, and limitation of OFF channels to negative contrast processing (Liang and Freed, 2010; Molnar et al., 2009; Werblin, 2010). We add evidence that ON cone bipolar cell axonal ribbons mediate crossover inhibition via synapses with both γ ACs and GACs, revealing network topologies not predicted from electrophysiology.

The GAC and γ AC targets are both mono- and multi-stratified (Figs. 7, 8). Both GAC and γ AC targets form feedback and feed-forward motifs, and γ AC targets also form nested feedback to axonal ribbons.

Given the extensive γ AC networks at bipolar cell axon terminals, it is not surprising that they engage axonal ribbons as well. γ AC feedback and nested feedback onto bipolar cells fine tunes bipolar cell presynaptic release (Marc and Liu, 2000) and is implicated in axonal ribbon release as well (Fig. 8C,H).

γ AC-mediated crossover inhibition via axonal ribbons (Fig. 8B,C right inset) extends the functional repertoire of γ ACs, demanding dissection of the potentially differential functional role of glycinergic and GABAergic crossover inhibition. Two nonexclusive functional implications arise. First, glycine receptor (glyR)-mediated, GABA_A receptor (GABA_AR)-mediated, and GABA_C receptor (GABA_CR)-mediated inhibition of bipolar cells may manifest different kinetics that combine with amacrine cell presynaptic release, such that GABA_AR- and glyR-mediated inhibition predominantly controls the magnitude of bipolar cell glutamate release, whereas GABA_CR-mediated inhibition controls the timing of bipolar cell glutamate release by increasing its transiency (Eggers and Lukasiewicz, 2006a,b, 2010, 2011; Eggers et al., 2007). Crossover inhibition networks may appropriate these kinetic differences to increase the range and complexity of bipolar cell and ganglion cell responses. Second, dual transmitters may optimize crossover inhibition by preventing synaptic occlusion, which occurs when two or more adjacent pre-

synaptic terminals release the same neurotransmitter onto a shared postsynaptic target (Fatima-Shad and Barry, 1992; Gold and Martin, 1984). The postsynaptic cell detects these multiple GABAergic synaptic inputs via the same type of GABA receptors, so adjacent GABAergic inputs cross-desensitize. Introduction of multiple neurotransmitters at these locations discretizes the signals, which may be necessary to effect crossover inhibition properly.

We now consider the functional role of dual transmitter-mediated crossover inhibition for the $\text{CBb} > \gamma\text{AC} \geq \text{CBa}$ motif (Fig. 8B,C right inset). Most OFF cone bipolar cells receive ON inhibition (Molnar and Werblin, 2007). Furthermore, OFF cone bipolar cells are dominated by glyR-mediated inhibition, although they also receive some GABA_AR-mediated inhibition, but little GABA_CR-mediated inhibition (Eggers and Lukasiewicz, 2011). This is quantitatively inconsistent with the dominance of γ AC inputs to CBa cells but qualitatively matches observed higher GAC convergence on CBa as opposed to CBb cells. Given the similarities between glyR- and GABA_AR-mediated OFF cone bipolar cell response kinetics in response to natural stimuli, there is no obvious kinetic advantage to the utilization of both to cross-inhibit OFF cone bipolar cells. Thus, dual γ AC-mediated and GAC-mediated bipolar cell $>$ amacrine cell \geq bipolar cell crossover inhibition networks may reduce synaptic occlusion rather than control OFF cone bipolar cell peak release. That said, examples of axonal ribbon-involved adjacent γ AC and GAC processes sharing postsynaptic targets remain to be found. Although axonal ribbon-mediated $\text{OFF} \geq \text{ON}$ GABAergic crossover inhibition has not been discovered in the OFF layer, it has been found in the ON layer between OFF cone bipolar cell telodendria and ON cone bipolar cells and is the topic of future articles.

Predicting the function of $\text{OFF} \geq \text{ON}$, dual transmitter crossover inhibition is less clear, because of some slight discrepancies in the literature. Eggers and Lukasiewicz (2011) report that murine ON cone bipolar cells possess similar levels of GABA_AR- and GABA_CR-mediated inhibition, and little or no glyR-mediated inhibition, whereas others report glycine-mediated crossover inhibition of ON cone bipolar cells (Molnar et al., 2009; Werblin, 2010). Presuming that glyR-, GABA_AR-, and GABA_CR-mediated inhibition all occur in rabbit ON cone bipolar cells, which is consistent with amacrine cell networks in RC1, dual glycine- and GABA-mediated crossover inhibition would afford control of both the peak amplitude and the degree of prolonged release in ON cone bipolar cells. Synaptic occlusion reduction could be an additional benefit of dual-transmitter crossover inhibition in these cells, but more analysis is needed to determine the frequency of adjacent γ AC and GAC inputs to common targets.

GAC- vs. γ AC-mediated cross-channel feedback and feed-forward inhibition

Many networks described in this article constitute axonal ribbon-mediated cross-channel feedback inhibition ($\text{CBb} > \gamma\text{AC} \geq \text{CBa}$ and $\text{CBa} > \text{GAC} \geq \text{CBb}$ motifs) and cross-channel feed-forward inhibition ($\text{CBb} > \text{GAC} \geq$ ganglion cell and $\text{CBa} > \text{GAC} \geq$ ganglion cell motifs). These motifs could also subserve kinetically appropriate ON-OFF response properties in polarity-opposite targets. Axonal ribbon reciprocal synapses can inject OFF components into ON channels, inject ON components into OFF channels, and construct ON-OFF target cells. GAC and γ AC feed-forward motifs discovered thus far are different. γ ACs feed-forward to targets also directly driven by axonal ribbons by the CBb, whereas GACs feed-forward to targets not directly driven by those axonal ribbons. We refer to these as “in-class” and “cross-class” feed-forward motifs, respectively. One common form of glycinergic ON \geq OFF crossover is provided by A_{II} AC lobular dendrite synapses onto OFF cone bipolar cells and extensive input to OFF α and δ ganglion cells. Neither A_{II} ACs nor OFF α/δ ganglion cells are targeted by ON cone bipolar cell axonal synapses, despite abundant opportunities.

The diversity of inputs to ON-OFF amacrine cells aligns with the complexity of amacrine cell/ganglion cell response properties. We show that an anatomical framework exists to support glycine- and GABA-mediated control of ON cone bipolar cell release at axonal ribbon locations, which may subserve both crossover inhibition and ON-OFF GAC regulation of ON cone bipolar cell axonal ribbon synapse release kinetics.

Rod bipolar cell axonal ribbons are distinct from ON cone bipolar cell axonal ribbons

Despite the fact that multiple groups have reported very few, if any, axonal ribbons in rod bipolar cells (Chun et al., 1993; Ghosh et al., 2001; Tsukamoto et al., 2001), our results are more consistent with those of Strettoi et al. (1990), who reported occasional instances of output synapses along the descending axons of rod bipolar cells. Nonetheless, the rod bipolar cell axonal ribbons all occur en passant, with no evident branching, and are concentrated in the ON IPL (Fig. 4). Those that breach the ON-OFF boundary do so marginally; they comprise ON drive to polarity-matched targets, distinct from ON-OFF cross-talk achieved by ON cone bipolar cell axonal ribbons in the rabbit retina. The absence of rod bipolar cell axonal ribbons in the distal OFF layer is significant in that M1 ipRGCs exhibit rod responses (Aggelopoulos and Meissl, 2000; Dacey et al., 2005; Wong et al., 2007). Possible sources include the primary A_{II} -mediated scotopic pathway, the secondary rod::cone coupling scotopic

pathway, or direct rod bipolar cell axonal synapses with M1 ipRGCs as suggested by Ostergaard et al. (2007). Our data demonstrate that rod input to M1 cells absolutely does not arise from rod bipolar cell axonal ribbons. Moreover, we have found no evidence of rod bipolar cell synapses onto ganglion cells of any type, and the rod bipolar cell axonal ribbons discovered thus far target only A_I and A_{II} ACs, both typical ON layer targets of rod bipolar cell ribbons. A_I AC rod bipolar cell axonal ribbon targets are further consistent with previous work demonstrating that A_I AC dendrites sometimes immediately appose GABA receptors on descending rod bipolar cell axons in the ON IPL sublaminae, expected for reciprocal synapses observed between A_I ACs and rod bipolar cell ribbons (Wässle et al., 1991; Zhang et al., 2002).

Multiple axonal synaptic and network topologies distribute functionality

Axonal ribbons routinely construct convergent and divergent synaptic motifs. The synaptic topologies vary across these examples, including all combinations of single- vs. multiple-ribbon and monadic vs. dyadic synapses (Figs. 6–9). Axonal ribbons also tend to be smaller than ribbons in the primary ON cone bipolar cell arbors. Distinct synaptic topologies are considered here.

First, $\text{CBb5w } 6156$ forms single-ribbon, monadic axonal synapses to drive an ipRGC and a narrow-field, diffusely stratified GAC employed for divergent within- and cross-channel inhibition motifs (Figs. 6C,G, 7D,H). Second, wide-field cone bipolar cell 5283 drives the ipRGC targeted by $\text{CBb5w } 6156$ with a multiribbon, monadic axonal synapse (Fig. 6C,H), demonstrating different synaptic topological input to a common target, albeit from two classes of ON cone bipolar cell. Third, $\text{CBb6 } 5536$ displays a single-ribbon, branched axonal synapse dyad to drive a pair of OFF layer, monostратified amacrine cell processes, which provide nested feedback to the CBb6 and one of which mediates $\text{CBb} > \gamma\text{AC} \geq \text{CBa}$ crossover inhibition (Fig. 8C right inset,H,I). Finally, $\text{CBb5 } 400$ forms a multiribbon, dyadic axonal synapse onto ganglion cell 5118 and a currently unidentified process (Fig. 6B,F).

No clear pattern emerges for the rules governing axonal ribbon synaptic topologies, but we can eliminate two possibilities. First, the target cell does not govern axonal ribbon count, as evidenced by the ipRGC recipient to convergent input from two axonal ribbon monads with different numbers of ribbons. Second, cone bipolar cell class does not govern axonal ribbon synaptic topology, given that ON cone bipolar cells of the same class can instantiate different axonal synaptic topologies (Fig. 6D,I–J,L), and ON cone bipolar cells of different classes

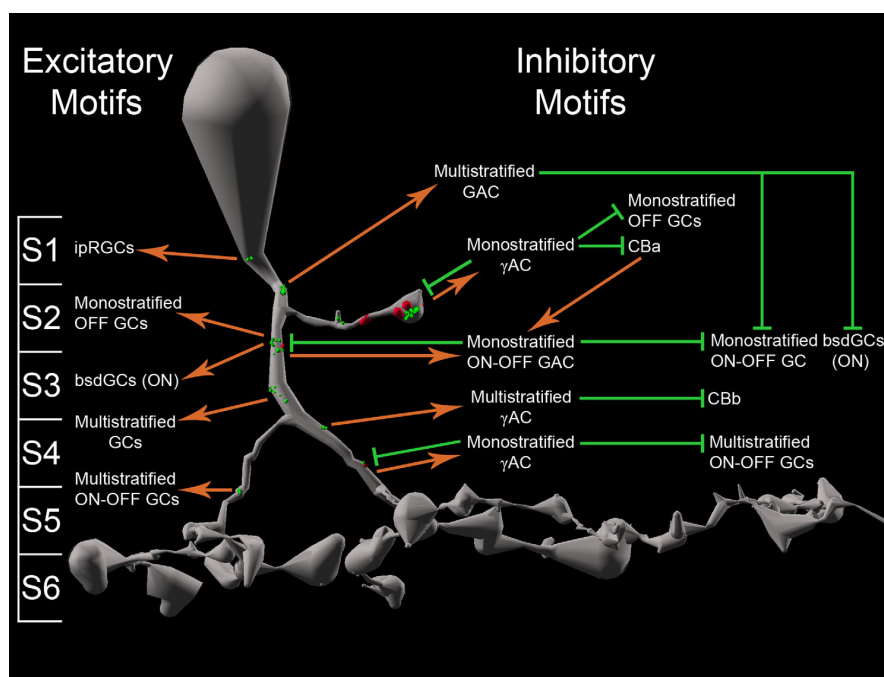


Figure 12. Axonal ribbon motifs summary semischematic. Wiring diagram for axonal ribbon motifs discovered across all cone bipolar cell classes in RC1 collapsed onto one representative cell. Spatial distributions of axonal ribbons have been preserved as well as possible to represent actual axonal ribbon locations. The axonal branch in sublamina 2 and the bifurcated descending axon are included for completeness, although both occur in a minority of cone bipolar cells. Note that, in addition to abundant axonal ribbon output, cone bipolar descending axons are frequently postsynaptic to amacrine cell inputs. S1–S6, IPL sublaminae 1–6; orange arrows, excitatory ribbon synapses; green arrows, inhibitory GAC- or γ AC-mediated synapses; GC, ganglion cell.

can share synaptic topologies (Fig. 6A,E,D inset,L). More source–target analysis is needed on this topic.

Monostratification achieves ON–OFF cross-talk via axonal ribbons

It is generally thought that ganglion cells acquire ON–OFF responses via bistratification across the ON and OFF IPL, yet in WT mice 11% of ganglion cells establish ON–OFF properties by P33 via monostratification of one thick band of dendrites in the middle IPL (Tian, 2008). Ganglion cell process 18693, targeted in CBB > ON–OFF GAC \geq ON–OFF ganglion cell crossover inhibition (Fig. 9B–D), is one such monostratified ganglion cell. Unfortunately, this ganglion cell process exits RC1, so we cannot verify that it lacks another stratum of arborization. However, its annotated processes co-stratify in the mid-IPL with GAC 906, from which it receives crossover inhibition, driven by an axonal ribbon (Fig. 9B,G). This example of co-monostratification of a GAC and ganglion cell in the same crossover inhibition network demonstrates that multistratified bipolar cells can mediate ON–OFF cross-talk. Moreover, it is now established that the entire OFF layer of the IPL contains mixed ON–OFF signal processing, so it fol-

lows that almost any monostratified cell could develop ON–OFF responses.

Axonal cisterns

Although the function of axonal cisterns is unknown, they are not randomly distributed and appear as well-ordered accessory ON network elements to common target cells. They are often in close proximity to axonal ribbon synapses (Fig. 6C,H), converge onto common targets (Fig. 6C,H,8B,K), and have been observed reciprocal to conventional synapses (data not shown), suggesting that they are real structural or communicative elements of accessory ON networks. Indeed, preliminary analyses reveal that 55 of 113 (48.7%) measured cone bipolar cells contain one or more axonal cisterns. More complete analyses will be conducted in the future.

Axonal ribbons are routine network elements throughout the IPL

Ten axonal ribbon-mediated network motifs have been discovered in RC1 thus far spanning all IPL sublaminae (Fig. 12), emphasizing their routine cone bipolar cell signaling. It is highly likely that additional motifs exist, because many axonal ribbon targets and networks remain to be

identified. The excitatory motifs provide direct axonal ribbon drive to an array of ganglion cell classes. The inhibitory motifs comprise both feedback and feed-forward as they target GACs and γ ACs, which in turn form synapses onto CBAs, CBbs, and several classes of ganglion cell.

Figure 12 collapses the network motifs reported here onto one representative cone bipolar cell for clarity. Two features that occur in a minority of cells are included, branched axonal ribbons in the canonical OFF IPL and bifurcated descending axons. It is important to distinguish between a bifurcated axon and the primary branch point of the telodendria. ON cone bipolar cell descending axon bifurcations occur in sublaminae 3–5, distinctly distal to the primary arborization of the cell. In such cases, the descending axon typically bifurcates into major (Fig. 12, right branch) and minor (Fig. 12, left branch) axons before each primarily arborizes. The major branch diameter remains comparable to the descending axon diameter distal to the bifurcation, whereas the minor branch point adopts a smaller diameter. Each branch retains axonal features such as predominant microtubule bundles and a scarcity of vesicles, except for vesicle clouds concentrated near axonal ribbons. In cases of clearly bifurcated descending axons distal to the primary arborization of the cell, such as that shown in Figure 12, ribbon synapses in both the major and the minor axons were still classified as “axonal.” Note that, in addition to abundant axonal ribbon output, cone bipolar descending axons are frequently postsynaptic to amacrine cell inputs, both reciprocal and nonreciprocal to axonal ribbons.

ACKNOWLEDGMENT

We thank James Tucker for assistance with imaging and discussions, and Hope Morrison for annotation of cells in the RC1 volume. The RC1 data set is freely available to be transferred to user media or viewed with the Viking application upon request.

CONFLICT OF INTEREST STATEMENT

Robert E. Marc is a principal of Signature Immunologics, Inc., manufacturer of some reagents used in this work.

ROLE OF AUTHORS

All authors had full access to all the data in the study and take responsibility for the integrity of the data and the accuracy of the data analysis. Study concept and design: JSL, REM. Acquisition of data: JSL, JVH, REM. Analysis and interpretation of data: JSL, REM. Drafting of the manuscript: JSL, REM. Critical revision of the manuscript for important intellectual content: JSL, REM. Statistical analysis: JSL, REM. Obtained funding: REM. Administrative, technical, and material support: JRA, BWJ, CBW, SM. Study supervision: REM.

LITERATURE CITED

- Aggelopoulos NC, Meissl H. 2000. Responses of neurones of the rat suprachiasmatic nucleus to retinal illumination under photopic and scotopic conditions. *J Physiol* 623: 211–222.
- Anderson JR, Jones BW, Watt CB, Shaw MV, Yang J, DeMill D, Lauritzen JS, Lin Y, Rapp K, Mastronarde D, Koshevoy P, Grimm B, Tasdizen T, Whitaker R, Marc RE. 2009. A computational framework for ultrastructural mapping of neural circuitry. *PLoS Biol* 7:e1000074.
- Anderson JR, Jones BW, Yang J-H, Shaw MV, Watt CB, Koshevoy P, Spaltenstein J, Jurrus E, Kannan UV, Whitaker R, Mastronarde D, Tasdizen T, Marc RE. 2011a. Exploring the retinal connectome. *Mol Vision* 17:355–379.
- Anderson JR, Mohammed S, Grimm B, Jones BW, Koshevoy P, Tasdizen T, Whitaker R, Marc RE. 2011b. The Viking viewer for connectomics: scalable multi-user annotation and summarization of large volume data sets. *J Microsc* 241: 13–28.
- Briggman KL, Bock DD. 2011. Volume electron microscopy for neuronal circuit reconstruction. *Curr Opin Neurobiol* 22: 1–8.
- Calkins DJ, Tsukamoto Y, Sterling P. 1998. Microcircuitry and mosaic of a blue-yellow ganglion cell in the primate retina. *J Neurosci* 18:3373–3385.
- Chavez AE, Diamond JS. 2008. Diverse mechanisms underlie glycinergic feedback transmission onto rod bipolar cells in the rat retina. *J Neurosci* 28:7919–7928.
- Chen X, Hsueh HA, Werblin FS. 2011. Amacrine-to-acacrine cell inhibition: spatiotemporal properties of GABA and glycine pathways. *Vis Neurosci* 28:193–204.
- Chun MH, Han SH, Chung JW, Wässle H. 1993. Electron microscopic analysis of the rod pathway of the rat retina. *J Comp Neurol* 332:421–432.
- Dacey DM, Liao HW, Peterson BB, FR R, Smith VC, Pokorny J, Yau KW, Gamlin PD. 2005. Melanopsin-expressing ganglion cells in primate retina signal colour and irradiance and project to the LGN. *Nature* 433:749–754.
- Dumitrescu ON, Pucci FG, Wong KY, Berson DM. 2009. Ectopic retinal ON bipolar cell synapses in the OFF inner plexiform layer: contacts with dopaminergic amacrine cells and melanopsin ganglion cells. *J Comp Neurol* 517: 226–244.
- Eggers ED, Lukasiewicz PD. 2006a. GABA_A, GABA_C, and glycine receptor-mediated inhibition differentially affects light-evoked signaling from mouse retinal rod bipolar cells. *J Physiol* 572:215–225.
- Eggers ED, Lukasiewicz PD. 2006b. Receptor and transmitter release properties set the time course of retinal inhibition. *J Neurosci* 26:9413–9425.
- Eggers ED, Lukasiewicz PD. 2010. Interneuron circuits tune inhibition in retinal bipolar cells. *J Neurophysiol* 103:25–37.
- Eggers E, Lukasiewicz P. 2011. Multiple pathways of inhibition shape bipolar cell responses in the retina. *Vis Neurosci* 28:95–108.
- Eggers ED, Lukasiewicz PD. 2007. Presynaptic inhibition differentially shapes transmission in distinct circuits in the mouse retina. *J Physiol* 582:569–582.
- Famiglietti EV. 1981. Functional architecture of cone bipolar cells in mammalian retina. *Vis Res* 21:1559–1563.
- Famiglietti EV, Kolb H. 1976. Structural basis for ON- and OFF-center responses in retinal ganglion cells. *Science* 194:193–195.
- Famiglietti EV. 1977. Neuronal Architecture of on and off pathways to ganglion cells in carp retina. *Science* 198: 1267–1269.
- Fatima-Shad K, Barry PH. 1992. A patch-clamp study of GABA- and strychnine-sensitive glycine-activated currents

- in post-natal tissue-cultured hippocampal neurons. *Proc Biol Sci* 250:99–105.
- Ghosh KK, Haverkamp S, Wässle H. 2001. Glutamate receptors in the rod pathway of the mammalian retina. *J Neurosci* 21:8636–8647.
- Gold MR, Martin AR. 1984. Gamma-aminobutyric acid and glycine activate Cl^- channels having different characteristics in CNS neurones. *Nature* 308:639–641.
- Graham D, Kolb H, Fernandez E, Nelson R. 2008. Melanopsin ganglion cells: a bit of fly in the mammalian eye. Webvision: The Organization of the Retina and Visual System [Internet]. Salt Lake City (UT): University of Utah Health Sciences Center; 1995–2008, August 1.
- Hoshi H, Liu W-L, Massey SC, Mills S. 2009. ON inputs to the OFF layer: bipolar cells that break the stratification rules of the retina. *J Neurosci* 29:8875–8883.
- Jeon CJ, Masland RH. 1995. A population of wide-field bipolar cells in the rabbit retina. *J Comp Neurol* 360:403–412.
- Kalloniatis M, Fletcher EL. 1993. Immunocytochemical localization of the amino acid neurotransmitters in the chicken retina. *J Comp Neurol* 336:174–193.
- Kolb H. 1982. The morphology of the bipolar cells, amacrine cells and ganglion cells in the retina of the turtle *Pseudemys scripta elegans*. *Philos Trans R Soc Lond B Biol Sci* 298:355–393.
- Kolb H. 1990. The synaptic organization of the dopaminergic amacrine cell in the cat retina. *J Neurocytol* 19:343–366.
- Kolb H, Cuenca H, Wang, Dekorver L. 1992. Neurons of the human retina: a Golgi study. *J Comp Neurol* 318:147–187.
- Liang Z, Freed M. 2010. The ON pathway rectifies the OFF pathway of the mammalian retina. *J Neurosci* 30:5533–5543.
- Linberg KA, Suemune S, Fisher SK. 1996. Retinal neurons of the California ground squirrel, *Spermophilus beecheyi*: a Golgi study. *J Comp Neurol* 365:173–216.
- MacNeil M, Heuss J, Dacheux R, Raviola E, Masland R. 2004. The population of bipolar cells in the rabbit retina. *J Comp Neurol* 472:73–86.
- Manookin MB, Beaudoin DL, Ernst ZR, Flagel LJ, Demb JB. 2008. Disinhibition combines with excitation to extend the operating range of the OFF visual pathway in daylight. *J Neurosci* 28:4136–4150.
- Marc RE. 1986. Neurochemical stratification in the inner plexiform layer of the vertebrate retina. *Vis Res* 26:223–238.
- Marc RE. 1999a. Kainate activation of horizontal, bipolar, amacrine, and ganglion cells in the rabbit retina. *J Comp Neurol* 407:65–76.
- Marc RE. 1999b. Mapping glutamatergic drive in the vertebrate retina with a channel-permeant organic cation. *J Comp Neurol* 407:47–64.
- Marc RE, Cameron DA. 2003. A molecular phenotype atlas of the zebrafish retina. *J Neurocytol* 30:593–654.
- Marc RE, Jones BW. 2002. Molecular phenotyping of retinal ganglion cells. *J Neurosci* 22:413–427.
- Marc RE, Jones BW, Lauritzen JS, Watt CB, Anderson JR. 2012. Building retinal connectomes. *Curr Opin Neurobiol* 22:568–574.
- Marc RE, Liu WL. 2000. Fundamental GABAergic amacrine cell circuitries in the retina: nested feedback, concatenated inhibition, and axosomatic synapses. *J Comp Neurol* 425:560–582.
- Marc RE, Murry R, Basinger SF. 1995. Pattern recognition of amino acid signatures in retinal neurons. *J Neurosci* 15:5106–5129.
- Mariani AP. 1982. Biplexiform cells: ganglion cells of the primate retina that contact photoreceptors. *Science* 216:1134–1136.
- Masland RH. 2001. Neuronal diversity in the retina. *Curr Opin Neurobiol* 11:431–436.
- McGuire B, Stevens J, Sterling P. 1984. Microcircuitry of bipolar cells in cat retina. *J Neurosci* 4:2920–2938.
- Molnar A, Werblin F. 2007. Inhibitory feedback shapes bipolar cell responses in the rabbit retina. *J Neurophysiol* 98:3423–3435.
- Molnar A, Werblin F. 2009. Crossover inhibition in the retina: circuitry that compensates for nonlinear rectifying synaptic transmission. *J Comput Neurosci* 27:569–590.
- Ostergaard J, Hannibal J, Fahrenkrug J. 2007. Synaptic contact between melanopsin-containing retinal ganglion cells and rod bipolar cells. *Invest Ophthalmol Vis Sci* 48:3812–3820.
- Pang JJ, Gao FF, Wu SM. 2004. Stratum-by-stratum projection of light response attributes by retinal bipolar cells of *Ambystoma*. *J Physiol* 558:249–262.
- Ramón y Cajal SR. 1892. La rétine des vertébrés. *Cellule* 9:121–225.
- Roska B, Werblin F. 2003. Rapid global shifts in natural scenes block spiking in specific ganglion cell types. *Nat Neurosci* 6:600–608.
- Roska B, Molnar A, Werblin FS. 2006. Parallel processing in retinal ganglion cells: how integration of space-time patterns of excitation and inhibition form the spiking output. *J Neurophysiol* 95:3810–3822.
- Scholes J. 1975. Colour receptors, and their synaptic connections, in the retina of a cyprinid fish. *Philos Trans R Soc Lond B Biol Sci* 270:61–118.
- Scholes J, Morris J. 1973. Receptor-bipolar connectivity patterns in fish retina. *Nature* 241:52–54.
- Sherry DM, Yazulla S. 1993. Goldfish bipolar cells and axon terminal patterns: a Golgi study. *J Comp Neurol* 329:188–200.
- Strettoi E, Dacheux RF, Raviola E. 1990. Synaptic connections of rod bipolar cells in the inner plexiform layer of the rabbit retina. *J Comp Neurol* 295:449–466.
- Tian N. 2008. Synaptic activity, visual experience and the maturation of retinal synaptic circuitry. *J Physiol* 586:4347–4355.
- Tsukamoto Y, Morigiwa K, Ueda M, Sterling P. 2001. Microcircuits for night vision in mouse retina. *J Neurosci* 21:8616–8623.
- Umino O, Maehara M, Hidaka S, Kita S, Hashimoto Y. 1994. The network properties of bipolar-bipolar cell coupling in the retina of teleost fishes. *Vis Neurosci* 11:533–548.
- Wagner HJ, Wagner E. 1988. Amacrine cells in the retina of a teleost fish, the roach (*Rutilus rutilus*): a Golgi study on differentiation and layering. *Philos Trans R Soc Lond B Biol Sci* 321:263–324.
- Wässle H, Puler C, Müller F, Haverkamp S. 1991. The rod bipolar cell of the mammalian retina. *Vis Neurosci* 7:99–112.
- Wässle H, Yamashita M, Greferath U, Grünert U, Müller F. 2009. Cone contacts, mosaics, and territories of bipolar cells in the mouse retina. *J Neurosci* 29:106–117.
- Werblin F. 2010. Six different roles for crossover inhibition in the retina: correcting the nonlinearities of synaptic transmission. *Vis Neurosci* 27:1–8.
- Werblin F, Dowling JE. 1969. Organization of the retina of the mudpuppy, *Necturus maculosus*. II. Intracellular recording. *J Neurophysiol* 32:339–355.
- Wong KY, Dowling JE. 2005. Retinal bipolar cell input mechanisms in giant danio. III. ON-OFF bipolar cells and their color-opponent mechanisms. *J Neurophysiol* 94:265–272.
- Wong KY, Dowling JE. 2007. Synaptic influences on rat ganglion-cell photoreceptors. *J Physiol* 582:279–296.
- Zhang J, Li W, Trexler EB, Massey SC. 2002. Confocal analysis of reciprocal feedback at rod bipolar terminals in the rabbit retina. *J Neurosci* 22:10871–10882.